

DEVELOPMENT OF A TIME RESOLVED FLUORESCENCE SPECTROSCOPY
SYSTEM FOR NEAR REAL-TIME CLINICAL DIAGNOSTIC APPLICATIONS

A Thesis

by

CHINTAN A. TRIVEDI

Submitted to the Office of Graduate Studies of
Texas A&M University
in partial fulfillment of the requirements for the degree of

MASTER OF SCIENCE

May 2009

Major Subject: Biomedical Engineering

DEVELOPMENT OF A TIME RESOLVED FLUORESCENCE SPECTROSCOPY
SYSTEM FOR NEAR REAL-TIME CLINICAL DIAGNOSTIC APPLICATIONS

A Thesis

by

CHINTAN A. TRIVEDI

Submitted to the Office of Graduate Studies of
Texas A&M University
in partial fulfillment of the requirements for the degree of

MASTER OF SCIENCE

Approved by:

Chair of Committee,	Javier A. Jo
Committee Members,	Brian E. Applegate
	Ronald D. Macfarlane
Head of Department,	Gerard L. Cote'

May 2009

Major Subject: Biomedical Engineering

ABSTRACT

Development of a Time Resolved Fluorescence Spectroscopy System for Near Real-Time
Clinical Diagnostic Applications. (May 2009)

Chintan A. Trivedi, B. E., Saurashtra University

Chair of Advisory Committee: Dr. Javier A. Jo

The design and development of a versatile time resolved fluorescence spectroscopy (TRFS) system capable of near real time data acquisition and processing for potential clinical diagnostic applications is reported. The TRFS apparatus is portable, versatile and compatible with the clinical environment. The main excitation source is a UV nitrogen laser with a nanosecond pulse width and the detection part consists of a dual grating spectrograph coupled with an MCP-PMT. The nitrogen laser also has a dye module attached to it, which enables broadband excitation of the sample. This setup allows rapid acquisition (250 ms for fluorescence decay at a wavelength) of time resolved fluorescence data with a high spectral (as low as 0.5 nm) and temporal (as low as 25 picoseconds) resolution. Alternatively, a state diode pumped pulsed laser can be used for excitation to improve data collection speed. The TRFS system is capable of measuring a broad range of fluorescence emission spectra (visible to near infra-red) and resolving a broad range of lifetimes (ranging from a few hundred picoseconds to several microseconds). The optical setup of the system is flexible permitting the connection of different light sources as well as optical fiber based probes for light delivery/collection depending on the need of the application. This permits the use of the TRFS apparatus in

in vitro, ex vivo and in vivo applications. The system is fully automated for real-time data acquisition and processing, facilitating near-real time clinical diagnostic applications.

DEDICATION

I would like to dedicate this work to my parents, family and friends. This work would not have been possible without my parents' encouragement and ever growing support. My friends and family members, who have always felt proud of my achievements and stood by me during my failures, deserve equal credit for this work.

ACKNOWLEDGEMENTS

First and foremost, I would like to thank my master's thesis advisor, Dr. Javier Jo. He has been everything that one could expect from an advisor. He has always been around to discuss problems related to research, and has helped me through some tough times, academically and otherwise. He has always encouraged insightful ideas or solutions that might come up during the discussions in the lab. I would also like to thank him for the financial support he has provided during the course of this work.

Secondly, I would like to thank my lab mates (Aditi, Patrick and Paritosh), who have been a constant source of help with my research. They have helped me analyze and discuss my results and without them, this work would not have been completed on time.

I would also like to acknowledge Bhavik Nathwani's support during my stay here at Texas A&M. He has always given me sound advice regarding all sorts of problems, and his encouraging words have helped harness my ever growing interest in research.

I would like to thank my friends and family living in the United States, who have not let me feel homesick in spite of my home being several thousand miles away. My cousins back home have always provided their support in my endeavors. Last, but not least, I would like to thank my parents. Without their support and fine upbringing, I would not have been able to follow this academic path.

TABLE OF CONTENTS

	Page
ABSTRACT.....	iii
DEDICATION.....	v
ACKNOWLEDGEMENTS.....	vi
TABLE OF CONTENTS.....	vii
LIST OF FIGURES	ix
LIST OF TABLES.....	x
INTRODUCTION AND MOTIVATION	1
BACKGROUND	4
Fluorescence Photophysics	4
Fluorescence Spectroscopy	7
Why Measure Fluorescent Lifetime?.....	10
Time Resolved Fluorescence Spectroscopy.....	12
Frequency Domain Time Resolved Fluorescence Spectroscopy.....	12
Time Domain Time Resolved Fluorescence Spectroscopy	14
Literature Review.....	16
Lifetime Kinetics and Analysis.....	18
Proposed System.....	21
METHODS	23
System Design	23
Light Sources	25
Light Delivery and Collection	26
Spectroscopy and Detection.....	27
Spectral and Temporal Resolution.....	28
System Synchronization.....	29
System Automation and Data Acquisition.....	31
Data Analysis	36
TRFS System Calibration	37
Validation of the TRFS System	38

	Page
RESULTS	41
Validation Results	41
System Performance	46
CONCLUSION, DISCUSSION AND FUTURE WORK.....	48
REFERENCES	52
APPENDIX A.....	58
APPENDIX B	60
APPENDIX C	62
VITA.....	63

LIST OF FIGURES

FIGURE	Page
1 Jablonski energy diagram	4
2 Block diagram of a steady state fluorescence spectrometer using right angle fluorescence detection.....	9
3 Time-domain and frequency-domain lifetime measurement approaches ...	12
4(a) TRFS system block diagram utilizing a bifurcated optical fiber bundle	24
4(b) TRFS system block diagram utilizing a side looking fiber attached to a dichroic filter setup	24
5(a) System timing diagram using 337 nm nitrogen laser for synchronizing the TRFS system.....	30
5(b) System timing diagram using 355 nm SPOT laser for synchronizing the TRFS system.....	31
6 Electrical diagram of the Time Resolved Fluorescence Spectroscopy (TRFS) system	32
7 Spectral calibration curve (350 - 800 nm)	38
8(a) Emission spectra of fluorescent dyes.....	42
8(b) Deconvolved Impulse Response Functions (IRFs) of fluorescent dyes	42
9(a) Emission spectra of biological fluorophores	43
9(b) Deconvolved Impulse Response Functions (IRFs) of biological fluorophores	43
10 Steady state emission spectra of a coronary artery sample.....	45
11 Deconvolution results for a fluorescence decay at 400 nm from an arterial sample.....	45

LIST OF TABLES

TABLE		Page
1	Excitation and emission maxima of endogenous fluorophores	8
2	Peak wavelengths and lifetime values of fluorescent dyes	44
3	Peak wavelengths and lifetime values of fluorescent biomolecules	44
4	Comparison of deconvolution results between 337 nm, 1 ns nitrogen & 355 nm, 1.3 ns Diode lasers	46
5	System performance results	47
6	Comparison of the present TRFS system with previous studies.....	49

INTRODUCTION AND MOTIVATION

Fluorescence spectroscopy and imaging have the potential to unravel biochemical and functional information about tissues.¹ This information can be interpreted to understand the biological processes governing several clinical problems. Fluorescence techniques have been explored for various clinical diagnostic applications primarily because they are noninvasive, easy to implement and provide quantitative information. Steady state fluorescence spectroscopy has been developed as a tool for in vivo detection of pre-cancer or cancer markers in various human organs such as bronchi,² bladder,³ breast,⁴ skin,⁵ colon,⁶ esophagus,⁷ brain,⁸ and oral cavity.⁹ It has also been applied for the in vivo detection of atherosclerotic plaques.¹⁰ However, steady state fluorescence spectroscopy carries certain inherent disadvantages when being applied to clinical studies. Most of the endogenous fluorophores have overlapping emission spectra¹¹ and this limits the specificity of steady state fluorescence as a tool for diagnosis. Moreover, spectral intensity in steady state fluorescence spectroscopy is affected by excitation-collection geometry, endogenous chromophores, transmission efficiency of optical paths and optical inhomogeneities in tissues making it difficult to obtain quantitative information regarding tissue biochemistry.¹²

This thesis follows the style of Review of Scientific Instruments.

Lifetime measurements are also independent of aforementioned intensity based parameters, thus rendering lifetime to be a more robust parameter to correlate to tissue biochemistry. The lifetime of a fluorophore is also sensitive to the biological micro-environment, thus providing more information about the tissue as compared to steady state fluorescence. Several groups have demonstrated the application of TRFS as a clinical diagnostic tool using different approaches.¹³⁻²⁰ The goal has been to develop a clinically compatible TRFS system that is user friendly, portable and capable of operating in near real-time in vivo. In spite of advances in instrumentation, time resolved fluorescence spectroscopy has not been implemented as a clinical tool for routine diagnostic procedures due to complex and expensive instrumentation and long data recording and analysis times.

The work presented in this study describes the design of a versatile Time Resolved Fluorescence Spectroscopy (TRFS) system for clinical diagnostic applications. To make the system compatible to a clinical environment, it will need to be user friendly, portable and capable of operating in near real time. Towards fulfilling this objective, three specific aims were proposed:

- Aim 1: To design, calibrate and validate a time resolved fluorescence spectroscopy system capable of measuring time resolved emission spectra for most desired ranges of endogenous and exogenous fluorophores
- Aim 2: To develop a GUI (Graphical User Interface) for the automation and control of the TRFS system facilitating real time data acquisition
- Aim 3: To implement an online data processing algorithm within the TRFS instrument to enable near real time data analysis

Development of a TRFS system that is compatible with a wide array of clinical applications and operates rapidly in near real time will facilitate the progress of TRFS towards the clinic. The proposed system has high spectral and temporal resolution, and is capable of real time in vivo measurements and data analysis, thus rendering it highly suitable for clinical applications. When TRFS needs to be applied as a clinical tool for in vivo applications, the amount of time that the system consumes to record and analyze the data is very critical. Real time measurement and online data analysis capabilities will ensure the feasibility of the TRFS system for in vivo clinical applications. Real time measurement and near real time data analysis will also provide instant information about the tissue biochemistry and hence help the clinician decide the future course of treatment. This report describes the design of the TRFS system, its calibration and validation using synthetic organic, biological fluorophores and biological tissues, its automation through a Graphical User Interface (GUI) and implementation of an online TRFS data analysis algorithm. The TRFS system performance in terms of speed and accuracy are also discussed along with its implications in clinical diagnosis.

BACKGROUND

In order to develop a time resolved fluorescence spectroscopy apparatus, it is important to understand the physical principles that govern fluorescence emission from a sample and determine its decay rate. This section will describe fluorescence photophysics and fluorescence lifetime decay kinetics. Time resolved spectroscopy implementation in both the time domain and frequency domain will be reviewed. Time-domain TRFS data analysis techniques and their pros and cons will also be covered in this section.

Fluorescence Photophysics

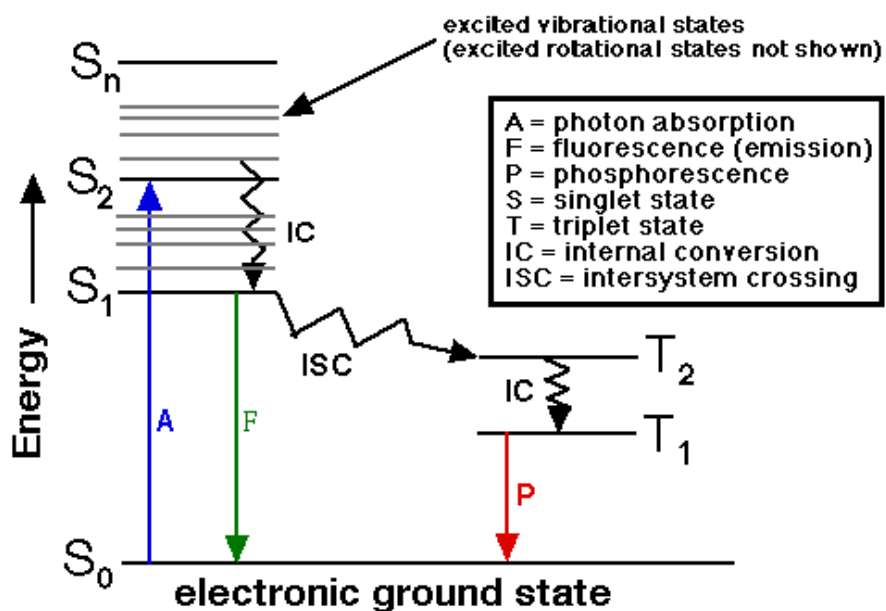


Figure 1: Jablonski energy diagram²¹ (Courtesy of Department of Chemistry, Sam Houston State University, Texas)

Luminescence is defined as the radiation emitted by an atom or molecule to move from the excited state to the ground state after absorbing energy. Fluorescence and phosphorescence are the types of luminescence observed. As shown in the Jablonski energy diagram in figure 1, S_0 is the ground state of a molecule, S_1 is the first excited state, S_2 is the second excited state and so on. A sample can be excited by various means putting the molecules in the sample into an electrically excited state, from which they can return to the ground state by several means. Fluorescence is a radiative decay through which the molecule can return to ground state. A fluorescent molecule absorbs energy and reaches an excited state and then loses it in the form of an emitted photon while returning to ground state. In fluorescent materials, the excited state has the same electron spin as the ground state. If A^* denotes an excited state of a substance A , then fluorescence excitation consists of the absorption of a photon of energy $h\nu_{ex}$.

$A + h\nu_{ex} \rightarrow A^*$, where h is Planck's constant, ν_{ex} is the frequency of the photon absorbed.

$A^* \rightarrow A + h\nu_{em}$, where ν_{em} is the frequency of the emitted photon.

Before a fluorescent molecule can emit a photon to decay to ground state, it needs to be at the lowest vibrational level of the excited state. This process of losing energy to get to the lowest vibrational level of the excited state is known as internal conversion or vibrational relaxation. Vibrational relaxation is a fairly quick process and occurs in a time scale of the order of 10^{-12} seconds. The photon emitted after internal conversion has lower energy and hence longer wavelength than the photon that was absorbed. This difference in energy or a difference in wavelength between the absorbed and emitted photon is known as Stoke's shift.

Fluorescence is usually observed as an average process for the entire molecular species. Hence a particular sample, where the molecular distribution is inhomogeneous, does not simply absorb energy at a specific wavelength or emit energy at a specific wavelength. Both absorption and emission occur over a range of wavelengths known as absorption and emission spectra respectively. These spectra represent the probability distribution over a range of wavelengths over which absorption/emission can occur. The average time which a molecule spends in the excited state before decaying to the ground state by emitting photons is known as the fluorophore lifetime. Lifetime is the exponential rate of decay of fluorescence emission with time. This process is usually of the order of 10^{-9} seconds.

There are several other processes apart from fluorescence through which a molecule in the excited state can lose energy. It can lose energy completely non-radiatively in the form of heat dissipation to the solvent. Excited molecules can also relax via conversion to a triplet state which may later relax via phosphorescence or by another non-radiative relaxation process. Electrons in a triplet state have the opposite spin than those in the ground state. Spin reversal and radiative decay from the triplet state to the ground state takes a fairly long time and hence phosphorescence is a process of the order 10^{-6} seconds, much slower than fluorescence.

The fluorescence intensity of a molecule is characterized by several other properties such as the molar extinction coefficient (i.e. the absorbing power) at the excitation wavelength, quantum yield (ratio of number of photons emitted to the number absorbed) at the emission wavelength and the concentration of the molecule in solution. A list of biological fluorophores, their excitation and emission peaks are described in

Table 1. Details of all endogenous fluorophores and their properties can be found elsewhere.^{11, 22} These endogenous fluorophores include amino acids, structural proteins, enzymes and co-enzymes, vitamins, lipids and porphyrins. Their excitation peaks lie in the range 250–450nm (UV/VIS spectral region),^{11, 22} whereas their emission peaks lie in the range 280–700nm (UV/VIS/NIR spectral region).^{11, 22} Different biological fluorophores are of interest when investigating various diseased conditions.²² For example, structural proteins such as collagen, elastin and lipoproteins are of interest when using fluorescence spectroscopy for atherosclerotic plaque detection, whereas NADH and FAD are important for cancer diagnosis.^{23, 24} Collagen fluorescence in load-bearing tissues is because of cross-links, hydroxylysyl pyridoline and lysyl pyridinoline.²⁵ The fluorescent material in elastin is a tricarboxylic triamino pyridinium derivative, which is very similar in spectral properties to the fluorophore in collagen.²⁶ Several other biological species of clinical importance can be probed using fluorescence spectroscopy to understand molecular processes occurring during the development and progression of these disorders.²⁷

Fluorescence Spectroscopy

The interaction of light with matter can result in several processes such as scattering, reflection, absorption and luminescence. Hence measurement of these processes at a molecular level can help identify the sample's molecular structure and chemistry.^{28, 29} Optical spectroscopy has been used as a tool to study these processes over a range of wavelengths and define a spectrum over which the sample under investigation is active. A typical steady state fluorescence spectrometer is shown in Figure 2. Steady

state fluorescence spectroscopy primarily consists of exciting the sample with a wavelength in the sample's excitation/absorption spectrum and measuring the intensity over the emission spectrum.

Table 1: Excitation and emission maxima of endogenous fluorophores

Endogenous fluorophore	Excitation maxima (nm)	Emission maxima (nm)
Amino acids		
Tryptophan	280	350
Tyrosine	275	300
Phenylalanine	260	280
Structural Proteins		
Collagen	325	400,405
Elastin	290,325	340,400
Enzymes and co-enzymes		
FAD, Flavins	450	535
NADH	290,351	440,460
NADPH	336	464
Vitamin B₆ compounds		
Pyridoxine	332,340	400
Pyridoxamine	335	400
Pyridoxal	390	480
Pyridoxic Acid	315	425
Pyridoxal 5'-phosphate	330	400
Vitamin B ₁₂	275	305
Lipids		
Phospholipids	436	540,560
Lipofuscin	340-395	540,430-460
Porphyrins	400-450	630,690

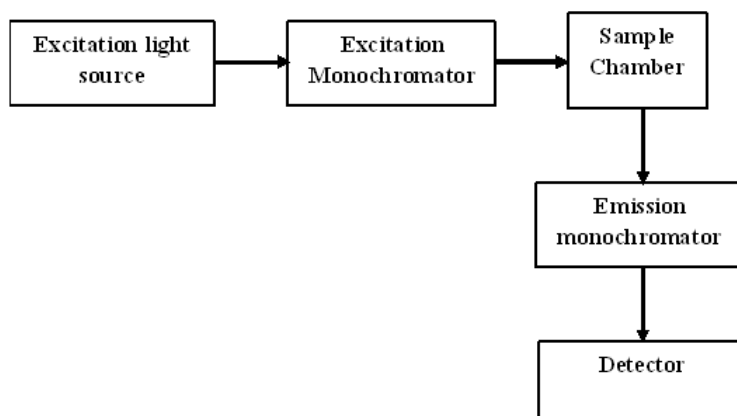


Figure 2: Block diagram of a steady state fluorescence spectrometer using right angle fluorescence detection

A steady state fluorescence spectrometer consists of a broad band continuous light source. The light source can be a Mercury or Xenon arc lamp, an incandescent lamp, or a QTH (Quartz tungsten halogen) lamp. To choose the excitation wavelength, an excitation monochromator is employed. Generally, monochromators have a concave diffraction grating with grooves that reflect each wavelength of light at a different angle. The selected excitation wavelength is focused by using lenses and made incident onto the sample. The fluorescence emitted is then directed towards an emission monochromator. The emission monochromator eliminates stray light and signal from the light source. To simplify the instrumentation or to make it inexpensive, long pass or band reject filters are placed instead of the emission monochromator. The emitted fluorescence light is now made incident onto the detector. PMT (Photo-multiplier tubes), photodiode or CCD devices are most often employed as detectors in a steady state fluorescence spectrometer.

The output of the detector is recorded by a computer at each wavelength in the emission spectrum and the data obtained is plotted on a graph of intensity or photon counts Vs wavelength.

Steady State fluorescence spectroscopy is an attractive tool for biomedical applications, because it is fast and non-invasive. In the UV/VIS spectral region, steady state fluorescence spectroscopy has been explored extensively as a diagnostic tool for precancer and cancer detection in various organs (colon,⁶ cervix,³⁰ bronchus,² bladder,³ brain,⁸ esophagus,⁷ skin,⁵ and breast⁴) and for the characterization of atherosclerotic plaques in cardio vascular tissues.¹⁰

Why Measure Fluorescent Lifetime?

Although steady state fluorescence spectroscopy is simple to implement, it suffers from several disadvantages. There are several biological fluorophores (Table 1) that have emission maxima fairly close to each other indicating that they have overlapping spectra. The fluorescence emission intensity measurements depend on several factors such as excitation and collection efficiency, transmission efficiency of optical paths, and optical inhomogeneities in tissues.²⁹ Since steady state measurements are intensity based, it becomes difficult to obtain absolute quantitative measurements that can be correlated to changes in tissue biochemistry. Steady state measurements are also affected by several molecular processes such as photobleaching,²⁸ quenching,²⁹ and other diffusive processes occurring in tissues.³¹ Photobleaching is the photodestruction of a molecule due to which it loses the ability to fluoresce and it usually occurs due to prolonged exposure of the sample to the light source. Loss of intensity in fluorescence emission due to

photobleaching, or quenching of fluorescence due to the presence of molecular quenchers such as oxygen³² in the tissue micro environment are difficult to interpret using steady state fluorescence.³³ Time resolved measurements measure the lifetimes of the fluorophores.

Time resolved measurements are independent of signal intensity and therefore independent of all artifacts that affect intensity based measurements as mentioned above. Biological components in tissues that emit fluorescence can be identified based on their unique lifetime value regardless of their emission spectra.^{34, 35, 36} For example, although collagen and elastin are spectrally overlapping, they can be distinguished from each other by their individual lifetime values. Collagen has an approximate lifetime of 1 – 1.5 nanoseconds, whereas elastin has an approximate lifetime of 2 – 2.5 nanoseconds.^{34, 35, 36} Photobleaching does not cause a change in lifetime, and hence time resolved fluorescence can be applied in spite of a loss in intensity.³⁷ Quenching can be monitored advantageously using time resolved measurements to understand molecular mechanisms as changes in lifetime are proportional to the rate of quenching processes^{38, 39}. Lifetime of a fluorophore is also sensitive to several other factors present in the biological microenvironment such as temperature,⁴⁰ pH,⁴⁰ ion concentration,⁴⁰ etc. Thus time resolved fluorescence spectroscopy can be a powerful tool for clinical applications in tissues since it is more robust as compared to steady state fluorescence spectroscopy and can provide more information.

Time Resolved Fluorescence Spectroscopy

Time resolved fluorescence spectroscopy can be performed in both time domain³⁰ and frequency domain.⁴¹ Fluorescence decay kinetics is interpreted differently in time domain and frequency domain. Although the decay is the same in both time and frequency domain, acquiring the fluorescence decay and then analyzing the data requires different approaches.

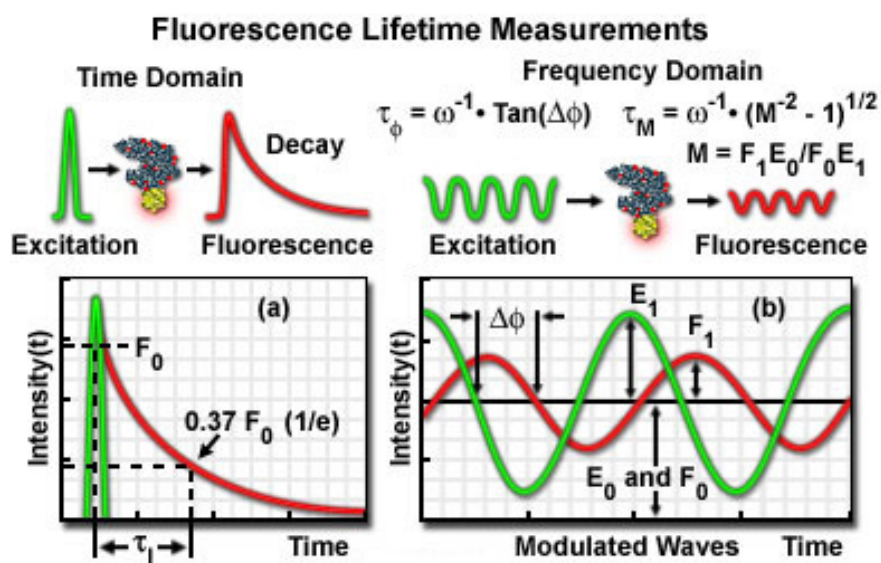


Figure 3: Time-domain and frequency-domain lifetime measurement approaches⁴² (Courtesy of Molecular ExpressionsTM, Optical Microscopy Primer)

Frequency Domain Time Resolved Fluorescence Spectroscopy

In the frequency-domain approach, a continuous laser acts as the excitation source. A high-power radio-frequency generator and an acousto-optical modulator sinusoidally modulate both source and detector, usually in the range of hundreds of MHz⁴¹ or even GHz.⁴³ Because of the time lag between the processes of absorption and emission, the detected fluorescence emission is also delayed in time and hence undergoes

a phase shift Φ_ω , where ω is the modulation frequency. The finite time response of the fluorophore (i.e. the lifetime) causes the emission intensity to be modulated by a factor of m_ω , compared to the excitation intensity. The amount of phase shift and modulation depend on the lifetime of the fluorophore and the modulation frequency. Detectors such as Avalanche Photo Diodes (APDs), Photo-multiplier tubes (PMTs) or Micro-Channel Plate Photo-multiplier tube (MCP-PMT) are employed for the detection of the sinusoidally modulated fluorescence signal.

Lifetime can be computed from the phase shift Φ_ω and the modulation m_ω ,

$$\tau_\Phi = (1/\omega) * \tan(\Delta\Phi_\omega)$$

$$\tau_m = (1/\omega) * [1 / (m_\omega^2 - 1)]^{1/2}, \text{ where } m_\omega = (F_1/E_0) / (F_0/E_1) \text{ as shown in Figure 3.}$$

For the exponential decay of a single component, τ_Φ and τ_m are equal and represent the apparent value of the lifetime. In the frequency domain, we must collect reference data, which typically consists of specular reflections from the laser source or a sample with a known lifetime, to estimate the detector's response.⁴⁴

Choosing the modulation frequency in frequency domain measurements is extremely important. For instance, if the excitation light is modulated at 2.0 MHz, a full cycle would be 500 nanoseconds long. Most biological fluorophores of interest in tissues have their lifetimes of the order of a few nanoseconds and at a time scale of 500 nanoseconds, the phase shift as well as modulated intensity would be barely visible. A modulation frequency of 20 MHz would mean a full cycle of 50 nanoseconds and 200 MHz would translate to a full cycle of 5 nanoseconds. In frequency domain measurements, the phase angle and modulation are measured over a range of modulation frequencies to obtain the frequency response of the sample.⁴¹ The frequency response

curve is generated by plotting phase angle versus wavelength and exponential models are used to fit the data. For clinical applications, the range of modulation frequencies is between 2-200 MHz.

Although frequency domain techniques are simple to implement, high speed electronics are required for modulation and detection, which increases the cost of frequency domain TRFS systems. Measuring phase and modulation over a wide range of frequencies, and extracting lifetime values through data analysis can be time consuming and computationally expensive.⁴⁵ Clinical applications require rapid real time measurements of time resolved spectra and hence frequency domain TRFS systems are less suitable for clinical diagnostics.

Time Domain Time Resolved Fluorescence Spectroscopy

In time domain fluorescence spectroscopy, the sample is excited with a pulsed light source, and the resulting fluorescence decay is recorded over time. The pulse width should theoretically be an impulse, but practically should be shorter than the expected decay of the sample. For measuring lifetimes of most biological fluorophores, pulse width of the order of a few hundred picoseconds or even a nanosecond is sufficient.

There are several approaches that can be used to implement time domain time resolved fluorescence spectroscopy. Although a pulsed laser is invariably used as an excitation source, different detection and acquisition schemes can be used according to the application. Time Correlated Single Photon Counting (TCSPC),⁴⁶ high speed time gated CCD devices,⁴⁷ streak cameras⁴⁸ and pulse sampling/transient recording through a high speed digitizer⁴⁹ are some of the time domain approaches that can be employed.

Each approach has varying spectral and temporal resolution with differing acquisition times.⁵⁰ Time correlated single photon counting (TCSPC) works on the principle that a single photon is detected for more than one excitation pulse. The delay time between that excitation pulse and the detection of the first photon is recorded. Each of these photons detected are stored in a histogram with the horizontal axis representing the delay between excitation pulse and detection of the first photon and the vertical axis representing the photon count at that specific delay interval. When the histogram has recorded a sufficient amount of photons (of the order of 10^6), it will represent the recorded decay. This technique requires high repetition rate picosecond or femtosecond lasers, high speed electronics for measuring delay intervals and a MCP-PMT (Micro Channel plate Photo Multiplier Tube) as the detector.⁴⁶ It is the most popular technique for time resolved measurements but other methods can be used when rapid measurements are required. Details on the TCSPC technique and its implementation can be found elsewhere.⁵¹ Streak cameras have been used for detection in time resolved fluorescence spectroscopy as well. Streak cameras can provide measurements of time resolved data with high temporal and spectral resolution simultaneously.¹ The streak camera operates on the principle of converting the temporal information of the pulse into the spatial domain. The pulse incident on the camera is made incident on a photocathode after being passed through a series of sweeping electrodes. Hence, photons arriving at different points in time are incident at different points on the detector. A grating placed in front of the slit of the streak camera can be used to select the desired wavelength, thus enabling simultaneous temporal and spectral detection. The temporal resolution of a streak camera is limited by the speed of the sweeping electrodes. The instrument response function of a streak

camera is superior to that of some of the fastest MCP-PMTs.¹ However, streak cameras are fairly expensive compared to MCP-PMTs. Pulse sampling or transient recording is another approach that has recently gained popularity for time resolved fluorescence spectroscopy in clinical applications.^{50, 52, 53} It allows recording of an entire decay with a single excitation pulse at a good signal to noise ratio. High speed digitizers or digital oscilloscopes can be used for the purpose of decay pulse sampling. High bandwidth detectors are used to record fluorescence intensity decay over time. With the advent of high speed digitizers and advanced MCP-PMTs, systems with high temporal and spectral resolution have been developed.^{50, 52, 53}

Literature Review

Time-Resolved Fluorescence Spectroscopy in the time domain has been evaluated as a clinical tool for in vivo diagnostic applications.¹³⁻²⁰ Several TRFS apparatus have been developed for clinical applications with the purpose of making the device portable, inexpensive, capable of performing near real time data acquisition and accurate data analysis. Glanzmann et al¹³ have demonstrated time domain TRFS on human bronchi, bladder and esophagus in vivo with rapid real time data acquisition (~20 seconds for an entire time resolved spectra of about 20 wavelengths) and sub nanosecond temporal resolution using a streak camera as a gated detector. The system consists of a pulsed laser source that is delivered through an optical fiber connected to an endoscope. A photodiode and an electrical delay unit is used to synchronize the acquisition of the signal with each laser pulse. Pitts et al¹⁴ have attempted a similar study on colonic polyps with fast data acquisition speeds but poorer spectral (~ 3 nm) and temporal resolution (~400

picoseconds). A dichroic mirror setup delivered the excitation light to the sample through a fiber and the collected light was diverted through the same setup to the detection system. A spectrograph connected to a gated ICCD was used as the detection system. Light sources used in both these studies were nitrogen lasers (337 nm wavelength) connected to dye laser modules to enable a broad range of excitation. Fang et al⁵⁰ have also demonstrated a time resolved fluorescence spectroscopy apparatus using a similar excitation light source, rapid acquisition times (~ 1 s for each decay), high spectral resolution (~0.5 nm) and sub nanosecond temporal resolution using an MCP-PMT and a high speed digitizer using the pulse sampling technique. Manning et al¹⁵ have developed a compact multidimensional fluorescence spectroscopy apparatus based on the time correlated single photon counting principle using ultra fast lasers based on the super continuum principle capable of providing excitation over the a portion of the UV, the entire VIS and NIR range. The system is capable of measuring lifetime, anisotropy, and excitation and emission profiles using a fiber optic probe. Lifetime data was obtained using a 16 channel PMT detector and each decay acquisition took approximately 2 seconds. Spectral resolution used was about 5 nm.

Time Resolved Fluorescence Spectroscopy (TRFS) has been applied to several clinical applications with varying levels of success. Mycek et al¹⁶ have demonstrated colonic polyp differentiation into adenomatous polyps (APs) and non adenomatous polyps (non-APs) during colonoscopy with high specificity (~91 %) through TRFS, which is comparable to routine clinical pathology studies. Glanzmann et al¹³ successfully characterized time resolved autofluorescence from human bronchi, bladder and esophagus and also differentiated between normal and neoplastic tissue autofluorescence

in these organs in vivo during endoscopy. Chen et al¹⁷ have applied TRFS to differentiate oral tissues into Normal Oral Mucosa (NOM), Epithelial Hyperplasia (EH), Verrucous Hyperplasia (VH), and Epithelial Dysplasia (ED) categories with an accuracy of 100 % for NOM, 75 % for VH and EH and 93 % for ED. Marcu et al¹⁸ have demonstrated through in vivo studies in animal models that time resolved fluorescence spectroscopy can be used to identify macrophage infiltration in atherosclerotic plaques, which is a key marker of plaque vulnerability. They have also shown that selectivity and specificity in identifying plaque composition increases when using time resolved fluorescence measurements as compared to steady state fluorescence spectroscopy alone.¹⁸ Marcu et al¹⁹ in a similar study done ex vivo on human arterial samples demonstrated the potential of TRFS as a tool to identify plaque biochemistry and detect rupture prone atherosclerotic plaques. Yong et al²⁰ have explored TRFS as a tool to characterize lifetimes and autofluorescence of normal brain tissue and glioma. They also differentiated between normal cerebral cortex regions and normal white matter, and could categorize gliomas into low grade glioma, high grade glioma and high grade glioma with necrotic change with reasonable accuracy using time resolved fluorescence parameters.

Lifetime Kinetics and Analysis

Data analysis techniques for time-domain TRFS methods will be reviewed and discussed here as the work reported in this study focuses on the implementation of a time-domain TRFS apparatus. A review on frequency domain data analysis approaches can be found elsewhere.^{54, 55}

Assuming the fluorescence decay to be a first order exponential, it can be represented as:

$I(t) = I_0 \cdot e^{-t/\tau}$ (1), where I_0 is the fluorescent intensity at the time of excitation, and τ is the excited state lifetime. However, often the fluorescence signal could be originating from a mixture or a complex medium. Thus, it can be multi-exponential and it is described as a sum of the exponentials:

$I(t) = I_0 \sum_{i=1}^n \alpha_i \cdot e^{-t/\tau_i}$ (2), where α_i is the contributing factor, and is a measure of the contribution of each exponential to the total fluorescence decay. τ_i is the individual decay time for exponential i .

Time resolved data analysis in the time-domain involves determination of the fluorescence decay parameter (also known as the fluorescence Impulse Response Function (IRF)). Impulse response function is the response of the system to an ideal delta (δ) excitation. However, excitation pulses are several picoseconds broad and hence the instrument response can be assumed to be a train of δ functions, each giving rise to an IRF. The sum of all the IRFs is the measured fluorescence decay. Mathematically, the measured fluorescence signal $y(t)$ is the convolution of the IRF $h(t)$ with the instrument response $x(t)$.⁵⁶ Deconvolution of the IRF from the excitation pulse allows us to estimate the true decay $h(t)$ and hence determine the lifetime.

$$y(t) = h(t) * x(t) \text{ (3)}$$

However, when using pulse sampling techniques, as in the design of the TRFS system in the work presented here, the fluorescence signal, the IRF as well as the excitation pulse are obtained in discrete time and hence expressed as $y(n)$, $h(n)$ and $x(n)$ respectively.⁵⁷ The equation can then be written as:

$y(n) = T \sum_{m=1}^{N-1} h(m) \cdot x(n - m) \dots$ (4), where $n = 0, 1, 2 \dots N-1$. N determines the number of samples, T is the sampling interval and $h(m)$ is the fluorescence IRF.

Ultra short pulses similar to the ideal δ function can be generated using femtosecond lasers and applied to time resolved fluorescence spectroscopy.⁵⁸ These light sources are expensive and since most of the endogenous fluorophores of interest have their lifetimes in the nanosecond range, it is feasible to use picosecond lasers for clinical applications. Picosecond lasers are readily available, portable and comparatively inexpensive. However, when using picosecond lasers for TRFS applications, accurate deconvolution of the IRF from the excitation pulse becomes very critical because several endogenous fluorophores have their lifetimes of the order of the excitation pulse width.⁵⁷

Deconvolution methods can be divided broadly into two groups⁵⁹: those that need an assumption of the functional form of the IRF, such as the nonlinear least-square iterative reconvolution (LSIR) method^{60, 61} and those that compute the IRF without any assumption about its functional form, such as the Fourier⁶² and Laplace⁶³ transform methods, the exponential series method⁵⁹, and the stretched exponential method.⁶⁴ A technique known as global analysis⁶⁵, in which simultaneous deconvolution of several fluorescence decay experiments are performed, has gained popularity for both time and frequency-domain TRFS data analysis. LSIR has been the most commonly used method for deconvolution of fluorescence data.^{13, 14, 16, 17} However, since it involves iterative convolutions, the method is computationally expensive and takes a fairly long time to produce the results. Additionally, different multi-exponential models can be fitted equally well to the same fluorescence decay.¹ Especially while analyzing tissue TRFS data, fluorescence emission might originate from several endogenous fluorophores, each

one representing either a single or a multi-exponential decay, resulting in complex decay dynamics.²² Hence when analyzing TRFS data from tissues, it is not appropriate to analyze fluorescence decays in terms of multi-exponential components because the resulting exponential terms cannot be directly correlated to some specific tissue fluorophore.⁵⁶ Thus, for tissue TRFS data analysis, it is advantageous to avoid any a priori physical model assumption of the fluorescence IRF.

A model free fast performing deconvolution technique based on discrete Laguerre Functions has been demonstrated for deconvolution of TRFS data.⁶⁶ Laguerre functions (LFs) have a built-in decaying exponential function and hence are appropriate for application to exponential dynamic systems. The Laguerre deconvolution technique uses the orthonormal set of discrete time LF $b_j^\alpha(n)$ to discretize and expand the fluorescence IRF:

$$h(n) = \sum_{j=0}^{L-1} c_j b_j^\alpha(n) \dots (5),$$
 where c_j are the unknown Laguerre expansion coefficients (LECs), which are to be estimated from the input output data; $b_j^\alpha(n)$ denotes the j 'th order orthonormal discrete time LF; and L is the number of LFs used to model the IRF.

Jo et al⁵⁷ have applied Laguerre deconvolution techniques for prediction of concentration of fluorophores in mixtures using Laguerre expansion coefficients (LECs). The Laguerre deconvolution technique has later been employed by the same group for data analysis in clinical applications such as time resolved fluorescence spectroscopy of atherosclerotic plaques¹⁸ and gliomas.²⁰ It was also shown in a study that LECs as a function of wavelength could be used to correlate specific changes in tissue biochemistry in atherosclerotic plaques.¹⁹

Proposed System

Pulse sampling techniques have recently gained popularity for clinical applications because they allow recording of a fluorescence decay curve with high temporal resolution using a single excitation pulse. High speed digitizers and gated detectors enable rapid data acquisition at a good signal to noise ratio. The TRFS apparatus reported in this work utilizes the pulse sampling approach for recording time resolved fluorescence spectra. A large effort has been focused on data analysis techniques for TRFS and several approaches to TRFS data analysis have been described. As mentioned previously, when analyzing time resolved fluorescence data from tissues, it is important to not make assumptions regarding the functional form of the IRF (Impulse response function). It is also important that the data analysis method be computationally fast and accurate. Laguerre deconvolution is one such technique that has been shown to be ultra fast in terms of time resolved data analysis and can provide information regarding underlying tissue biochemistry without any assumptions regarding the IRF. Hence, a Laguerre deconvolution algorithm capable of near-real time data analysis has been integrated into the TRFS system described in this work. Pulse sampling and Laguerre deconvolution based data analysis are both aimed at improving the system performance in terms of speed and accuracy.

METHODS

System Design

The time-resolved fluorescence spectroscopy (TRFS) system consisted of a light source for exciting the sample, a dual grating spectrograph cum monochromator for selecting the wavelength of interest, an MCP-PMT (Micro Channel Plate Photomultiplier Tube) for measuring the fluorescence decay, a high speed digital oscilloscope for sampling and recording data and a delay generator for synchronizing the system. The excitation light is coupled into an optical fiber and delivered to the sample. This induces fluorescence in the sample which is coupled into the collection fiber path and directed towards the monochromator. The motorized grating in the monochromator allows us to select the wavelength of interest and the fluorescence decay signal at this wavelength is detected by the MCP-PMT. The operation of the spectrograph as a scanning monochromator provides with the capability to measure time resolved emission spectra for the sample. The digital delay generator is used to send pulses to trigger the light source, and after a specific delay that equals the delay of the optical path, send pulses to gate the MCP-PMT as well the scope for detection. Figure 4 (a) shows the block diagram of the TRFS system setup using a bifurcated optical fiber bundle. Figure 4 (b) shows the block diagram of the TRFS system using a single side looking fiber attached to a dichroic filter setup.

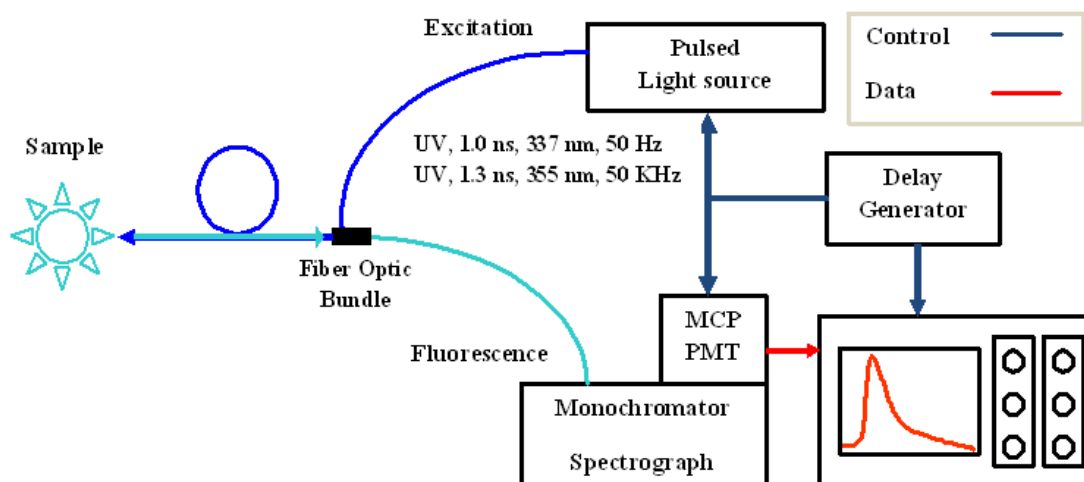


Figure 4 (a): TRFS system block diagram utilizing a bifurcated optical fiber bundle

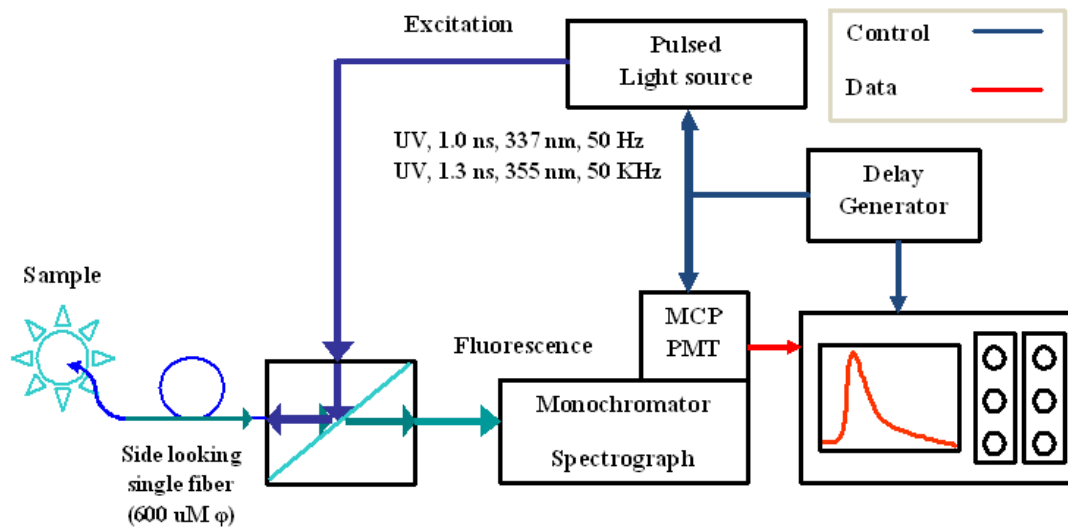


Figure 4 (b): TRFS system block diagram utilizing a side looking fiber attached to a dichroic filter setup

Light Sources

For the TRFS system presented in this work, a pulsed UV laser has been used. The excitation light source is a UV nitrogen laser connected to an auto-tuning dye module (MNL 200 LaserTechnik, Berlin, Germany). The fundamental wavelength of the laser is at 337.1 nm and the pulse width measured at full-width half-maximum was found to be 1 nanosecond. The maximum repetition rate for the laser is 50 Hz and the energy at the laser outlet was found to be 27 $\mu\text{J}/\text{pulse}$. The energy at the fiber tip was attenuated to 5 $\mu\text{J}/\text{pulse}$. It is important to control the energy per pulse specifically for clinical applications because high amounts of laser irradiance can have damaging effects on tissues. An energy level of 5 $\mu\text{J}/\text{pulse}$ at a 50 Hz repetition rate is within the permissible limits of laser irradiation for tissues. The laser has a low jitter (\pm 40 picoseconds) signal. High jitter content in the laser pulse can cause disruption of system timing and hence inaccurate measurement of fluorescence decays. The auto tuning dye module coupled to the nitrogen laser could be used for exciting different dyes provided by the manufacturer to obtain laser wavelengths over a broad range (400 – 950 nm). This provides capability to excite in UV-VIS range as well as a small portion of the NIR range.

The second excitation light source is a UV-VIS solid state diode pumped pulsed laser (ELFORLIGHT, SPOT laser). The laser's fundamental wavelength is tuned at 1064 nm and provides second harmonic pulses at 532 nm and the third harmonic pulses at 355 nm. The light source provided a low jitter (\pm 40 picoseconds) signal. The laser has been customized so as to provide 355nm at its output. The measured pulse width at full width half maximum was found to be 1.3 nanoseconds at 355 nm. The energy at the laser outlet was measured using a energy meter and it was approximately 6.5 $\mu\text{J}/\text{pulse}$ at 355 nm. The

laser can be operated at repetition rates as high as 50 KHz. However, the pulse width broadens and the energy per pulse decreases as the repetition rate is increased. Hence, the laser operation is limited to approximately 15 KHz, over which both the pulse width and the energy per pulse remain stable.

Light Delivery and Collection

The TRFS system design permitted the flexible use of various kinds of optical fibers for light delivery to the sample and collection of fluorescence emission from the sample. Two kinds of optical fiber probe designs were tested. The first probe is a custom-made bifurcated optical fiber bundle with a central excitation fiber about 600 μm in diameter surrounded by an array of fourteen 200 μm diameter collection fibers. The probe end is designed as a tip that can be held by hand during ex vivo or in vivo measurements from tissues. The excitation light from the laser is coupled into one arm of the bundle using an SMA connector. The light is delivered to the sample site and the fluorescence being emitted is collected by the collection fibers in the fiber bundle. These set of fibers merge into a single arm at the bifurcation joint and deliver light to the monochromator for spectroscopic detection. The fiber optic probe is sterilizable rendering it appropriate for clinical use.

The second optical fiber setup that was tested consists of a side looking single fiber about 600 μm in diameter customized for ex vivo and in vivo applications. An optical fiber connected to the pulsed excitation source delivers light to a dichroic filter setup as shown in figure 4. The dichroic filter reflects UV light but allows visible light to pass through. The reflected UV light is then made to enter the side looking fiber to excite

the sample, and the fluorescence emitted from the sample is collected by the same fiber and directed to dichroic filter setup. The dichroic filter allows the visible fluorescence to pass through to an optical fiber connected to the monochromator. Since only a single fiber is used in this setup instead of a fiber bundle, it allows the deployment of small diameter fiber optic probes for time resolved fluorescence studies, which is more suitable for clinical applications.

Spectroscopy and Detection

The collected fluorescence was directed to a 140 mm focal length dual grating spectrometer (MicroHR, Horiba Jobin Yvon). The spectrometer turret comprises of 1200 groves/mm grating on one side and a mirror on the other. The spectrometer can operate in the monochromator mode with a motorized grating that provides automated scanning ability over a spectrum with high resolution (as low as 0.5 nm). The resolution can be controlled manually with micrometer precision by controlling the size of entrance and exit slits. The spectrometer can also be operated in the spectrograph mode by changing the turret position to mirror and using band pass filters to obtain the average fluorescence signal over an entire band of wavelengths. Operating the spectrometer in the spectrograph mode allows the application of the system where signal levels are relatively low. An integrated signal for the entire band of wavelengths can provide a good signal to noise ratio as compared to the decay at a single wavelength in low amplitude signal conditions. The filters can be easily fitted in a five-position motorized filter wheel that can be automatically controlled as well. The filters in the filter wheel can be easily replaced depending on the need of the application.

The fluorescence emission at each specific wavelength as chosen by the monochromator is temporally detected by a gateable, variable gain Micro-channel plate Photo-multiplier tube (MCP-PMT, Hamamatsu, R5916U-50). The MCP-PMT has a rise time of 180 ps and a spectral response of 160 – 850 nm, thus enabling high resolution temporal detection and covering a broad spectral range. The MCP-PMT is coupled to a pre-amplifier (BW: 50 KHz – 1.5 GHz; C5594, Hamamatsu) which improves the signal to noise ratio during detection. The MCP-PMT gain can be controlled by a variable high voltage power supply (H556, Ortec, 0-3 kV). The output of the preamplifier is sent to a high speed digital oscilloscope (DPO7254, Tektronix, 2.5 GHz, 40 GSamples/sec). The digital oscilloscope doubles as the computer workstation thus eliminating the need for a separate console. The digital oscilloscope allows sampling at a resolution as low as 25 picoseconds and can be easily interfaced for automated real-time acquisition.

Spectral and Temporal Resolution

The spectral resolution of the system could be set manually from the monochromator/spectrograph by varying the entrance and exit slit width. The slit width can be adjusted using a micrometer screw. The minimum possible resolution is 0.4 nm with the slit width set at 80 μm and the maximum possible resolution being 21 nm with the slit width set at 4.0 mm. The slit width was set at 200 μm , which provided a spectral resolution of 2.6 nm approximately and at the same time let sufficient light to be incident on the detector to have a good signal to noise ratio. While acquiring time resolved spectra with the TRFS system, a step size of 5 nm is usually appropriate to resolved spectral

features and also enables faster acquisition of spectra. Hence, the resolution of the spectrograph set at 2.6 nm was found to be appropriate for clinical applications.

The temporal resolution can be adjusted by varying the sampling rate of the digital oscilloscope. The scope's sampling rate could be varied over a wide range, with a maximum of 40 GSamples/sec allowing temporal resolutions from a minimum of 25 picoseconds to several milliseconds. Generally for biological fluorophores, a resolution of 50 ps, 100 ps or 200 ps is appropriate and hence the user interface in the TRFS system let the user select one of these three options. A temporal resolution of 100 picoseconds is set as the default.

System Synchronization

There are several components in the system that can influence the system timing. These sources include: (a) electronic delays and jitter in the laser pulse (b) the detector gate width and (c) optical delays due to propagation of light through varying path lengths. Hence, it is important to have accurate knowledge of these parameters in order to synchronize the system for optimal detection. Synchronizing the system can assure the arrival of fluorescence at the detector when its gate is open. In order to synchronize the system, it is essential to synchronize the triggering of the excitation pulse, the gating of the detector and the triggering of the digitizer.

A 4-channel digital delay generator (Highland Technology, P400) serves the purpose of synchronizing the system operation. One channel is used to trigger the light source to generate a pulse. The optical delay of the path length was measured at about 1200 nanoseconds and this delay is used between the first and the second channel. The

second channel generates a pulse after this delay to gate the detector. The gate width is maintained at 500 nanoseconds in order to enable a sufficient window for fluorescence detection. While using different light sources, the synchronization system triggering the scope for acquisition may vary. When using the MNL 200, nitrogen laser, a trigger from the delay generator causes the laser to emit a pulse. A synchronized electrical pulse is also generated by the laser at the same time, which is then used to trigger the scope for acquisition of data. The system timing diagram is shown in Figure 5 (a), which gives an idea of system synchronization when using the nitrogen laser.

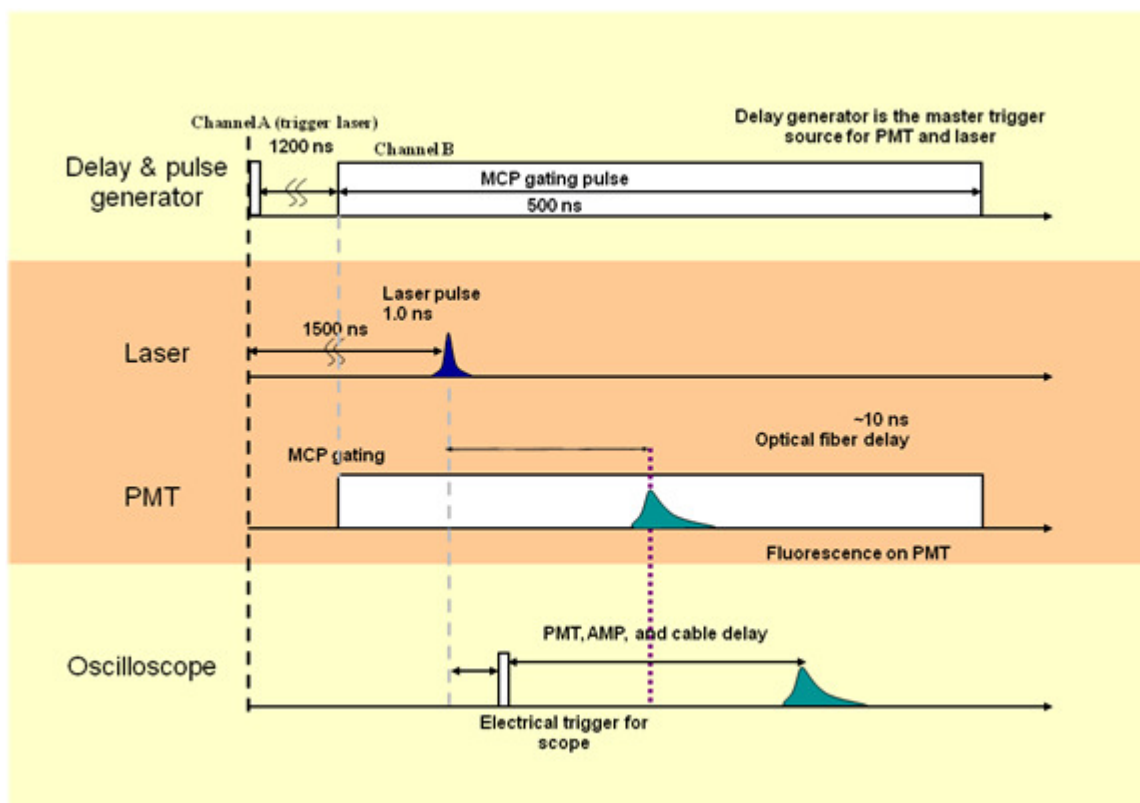


Figure 5 (a): System timing diagram using 337 nm nitrogen laser for synchronizing the TRFS system

Figure 5 (b) shows the system timing diagram for the SPOT (355 nm) light source. Since the SPOT laser does not have an electrical trigger generated, an additional channel from the digital delay generator is used to trigger the scope for acquisition. This pulse from the digital delay generator is delayed with respect to the trigger for the laser.

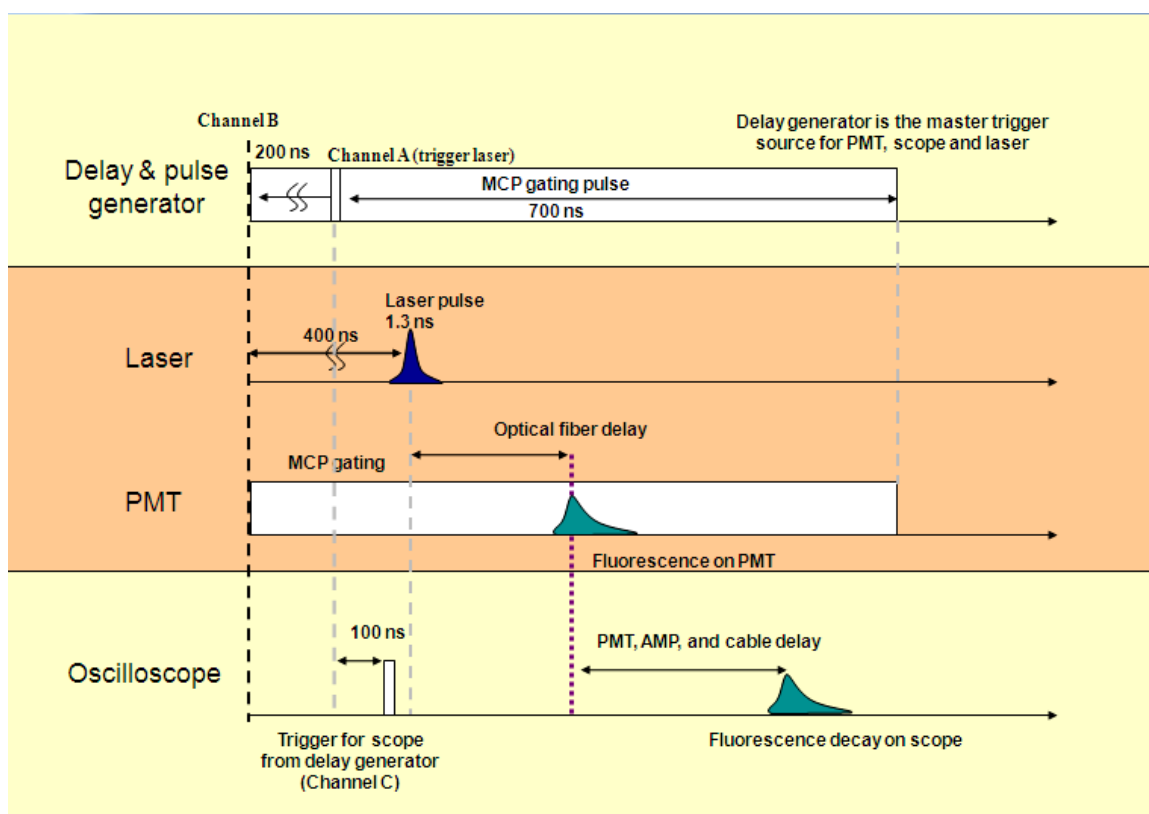


Figure 5 (b): System timing diagram using 355 nm SPOT laser for synchronizing the TRFS system

System Automation and Data Acquisition

The system is fully automated for real time data acquisition. Each component in the system is interfaced to the PC scope to enable automatic control. The laser is

connected to the PC scope through a serial port, the monochromator through a USB port, the digital delay generator through an Ethernet port, the oscilloscope to itself via a virtual GPIB (General Purpose Interface Bus) port and the power supply to control the gain of the MCP-PMT is connected to the scope via a GPIB port. Figure 6 shows the electrical interconnections and the interface paths of each component in the system to the computer workstation. This enables fully automated control as well as synchronized operation of the system.

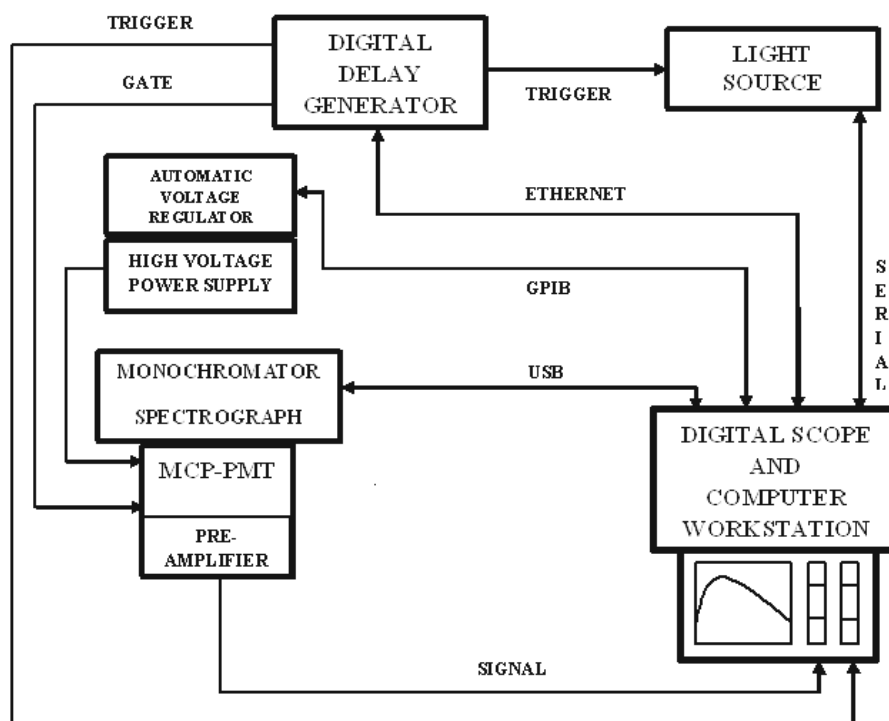


Figure 6: Electrical diagram of the Time Resolved Fluorescence Spectroscopy (TRFS) system

The data acquisition software was developed in LabVIEW™ graphical programming language (National Instruments Inc., Texas). The Graphical User Interface (GUI) was developed to provide individual control to each of the system components through the computer as well as to allow the user to choose acquisition parameters and automate the acquisition process. Data acquisition through the GUI consists of four basic steps:

- (1) Initializing all the system components.
- (2) Choosing the type of data acquisition and setting up acquisition parameters through the interface.
- (3) Perform real time data acquisition and automatically store the data in an organized manner.
- (4) Perform online data processing.

The interface allows the user to operate the system in three different modes. All the three modes allow the user to choose the laser repetition rate, the PMT gain, number of averages (default of 16 averages) of the signal before acquisition (averaging will assure a good signal to noise ratio for the decay signal that is being acquired), the desired filter at which the acquisition is to be done, the temporal resolution at which the data is to be recorded and the file name under which the data is to be saved. The user interface provides an option to let the user select whether an instrument response is to be recorded or not. An instrument response is measured as the backscattering of the laser pulse from the sample. It is used for deconvolution of the IR (Instrument Response) from the recorded fluorescence signal. Details on instrument response and its application in data analysis have been discussed in the data analysis subsection. It also allows the user to

preview the signal in real time at desired wavelengths before confirming acquisition. The three acquisition modes are described below.

(1) Discrete Wavelength Acquisition Mode: The discrete wavelength mode allows the user to choose and record decays at up to 5 discrete wavelengths. This mode is useful when the region of interest in the spectrum is known, and fluorescence decays at certain discrete wavelengths are needed for obtaining lifetime information which might be sufficient for a specific clinical application. This mode will enable rapid acquisition of data during in vivo applications.

(2) Spectral Acquisition Mode: The spectral mode allows the user to choose a spectrum of wavelengths over which decays are acquired. The mode also lets the user decide the step size between consecutive wavelengths and hence control the resolution of the spectrum. This mode is useful for complete characterization of time resolved fluorescence spectra of samples.

(3) Filter Wheel Acquisition Mode: The filter wheel mode allows the user to choose up to five different filters for acquiring average fluorescence decay over an entire band of wavelengths. The grating automatically moves to the mirror position during this mode thus letting the entire band of wavelengths passing through the filter to be detected as a single average decay. The filter wheel mode enables rapid determination of the region of interest in the fluorescence spectrum of a sample. This mode is beneficial when signal levels from the sample are fairly low. Data acquisition through the discrete wavelength mode in that case would deteriorate the signal. On the other hand, data acquired through the filter wheel mode would be an integration of the signal over the entire band of wavelengths, thus improving the signal to noise ratio as compared to the same for a single

wavelength. Moreover, the filters on the filter wheel can be easily replaced to modify the TRFS apparatus for different clinical applications or to cover different spectral ranges.

The filters that were installed in the filter wheel for the TRFS apparatus are listed below:

- (1) 337 +/- 5 nm notch filter + Neutral Density filter
- (2) 360 nm long pass filter
- (3) 400 +/- 20 nm band pass filter
- (4) 450 +/- 22 nm band pass filter
- (5) 500 +/- 22 nm band pass filter

The 337 nm notch filter is used for measuring the scattering of the laser pulse, which is used as the instrument response (IR) for deconvolution of decays. The ND (Neutral Density) filter attached with the notch filter assures that high intensity laser scattering does not saturate the PMT. The 360 nm long pass filter is used for acquisition of fluorescence spectra in the entire visible range, while blocking the laser scattering. This filter is most often chosen during the spectral acquisition mode. The other three filters (400,450 and 500 nm band pass) cover the broad range of visible emission that biological fluorophores usually emit. These filters are used in the filter wheel mode to acquire average fluorescence decays over a band of wavelengths.

After acquisition in each mode, collected data will be preprocessed for analysis and saved into sorted variables in a folder. The folder will also contain a file where all the acquisition parameters have been saved.

Data Analysis

The fluorescence decay signal recorded by the TRFS system is a convolution of the IR (Instrument Response) with the actual fluorescence decay.

It can be represented mathematically as:

$y(t) = h(t) * x(t)$; where $y(t)$ is the measured fluorescence decay, $h(t)$ is the fluorescence impulse response function and $x(t)$ is the instrument response. To measure the instrument response $x(t)$, the laser pulse backscattered from the sample is usually recorded. To record the instrument response (IR), the GUI directs the spectrograph to shift to 337 nm as the acquisition wavelength. The filter position is then switched to the notch (337 nm) + ND (neutral density) filter and the laser scattering is recorded. This is saved in the data file as the instrument response and later used for deconvolution. The TRFS system will provide automatic recording of the instrument response and store it for deconvolution of the time resolved data.

Several techniques have been implemented previously for deconvolution of time resolved fluorescence data.⁵⁹⁻⁶⁶ Least Squares Iterative Reconvolution (LSIR)⁶⁰ has been the most popular techniques for TRFS data analysis. However, LSIR has been found to be a computationally expensive tool. It has also been shown that when analyzing time resolved data from biological tissues, the decay dynamics can be complex⁵⁷. Hence, any assumptions regarding the functional form of IRF should be avoided. Several techniques based on multi exponential fits of the fluorescence decay have been proposed. However, different multi exponential models can be fitted to the same fluorescence decay, which would conceal the underlying information about tissue components emitting the fluorescence. A model free deconvolution technique, which does not make any a priori

assumptions regarding the functional form of IRF, based on orthonormal Laguerre functions has been proposed⁶⁶ and utilized for data analysis in TRFS applications.^{52-54,57}

For the TRFS instrument proposed in this study, an algorithm based on the Laguerre deconvolution technique was implemented and integrated with the GUI. This allowed near-real time data analysis as soon as the time resolved data was acquired. An online deconvolution algorithm has not been implemented before in time resolved fluorescence spectroscopy systems.

TRFS System Calibration

The TRFS system has components such as the optical fiber, the monochromator and the MCP-PMT, each of which has its own spectral response. The combination of these spectral responses can cause the signal intensity detected at a specific wavelength to be deviant from its actual wavelength. Hence, spectral intensity calibration is necessary to assure accurate measurement of time resolved spectra.

Spectral calibration was performed using a NIST traceable QTH (Quartz Tungsten Halogen) lamp (63358, Oriel). The calibration lamp had a broad emission over the entire visible spectrum, and the emission plot was provided by the manufacturer. A spectral correction factor $C(\lambda)$ was determined as a function of wavelength. This spectral correction factor $C(\lambda)$ was obtained by dividing the signal intensity of the calibration lamp measured by the system as a function of wavelength, $I(\lambda)$ by the corresponding signal intensity provided by the manufacturer $L(\lambda)$. The spectral correction factor can be represented as: $C(\lambda) = I(\lambda) / L(\lambda)$. Thus, a spectral correction curve was obtained, which was applied to all the measured emission spectra to correct for the spectral response of

the system. Figure 7 shows the spectral correction or the spectral calibration curve. The spectral calibration curve was incorporated in the GUI to correct the time resolved spectra that were acquired from a sample.

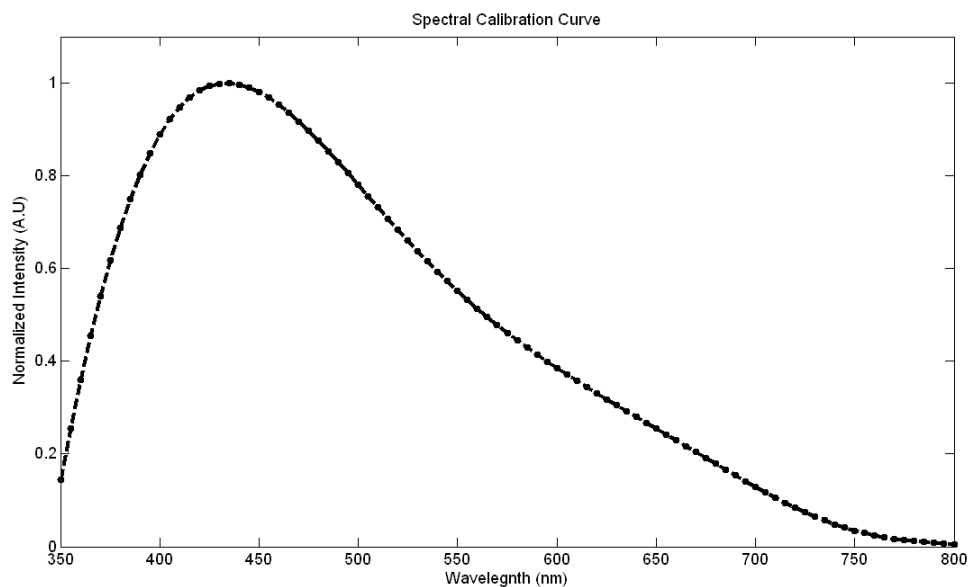


Figure 7: Spectral calibration curve (350 - 800 nm)

Validation of the TRFS System

The performance of the TRFS system both in terms of its spectral and temporal attributes was validated using standard fluorescent dyes and fluorescent biomolecules. Organic fluorescent dyes whose spectra and lifetime had been well characterized in literature previously were chosen for validation of the TRFS system. Since the TRFS system's primary application was for clinical studies, several biological fluorophores found both at the cellular and tissue level, were also used for validation.

Standard Fluorescent Dyes

The synthetic dyes were chosen so as to cover a broad spectral range (370 – 650 nm) and a broad range of lifetimes (500 ps – 12 ns). The dyes that were chosen for the experiments are easily available from the market in powder form. Rose Bengal (33,000, Sigma-Aldrich), Rhodamin B (25,242, Sigma-Aldrich) and 9-Cyanoanthracene (15,276, Sigma-Aldrich) were chosen for TRFS system validation. Stock solutions having concentration of the order of 10^{-3} M were prepared by adding appropriate amount of the powder dyes to their respective solvents. These solutions were then diluted to obtain concentrations of the order of a few tens of 10^{-6} M. For each sample, the time resolved spectra were obtained from 370 – 650 nm in increments of 5 nm each. The temporal resolution used for Rose Bengal and Rhodamin B was set to 100 picoseconds and 200 picoseconds for 9-Cyanoanthracene. Each of the samples was pipetted into a 1 cm x 1cm quartz cuvette and the fiber optic probe tip was held against the cuvette for measurements. The instrument response (IR) was automatically recorded by the TRFS GUI at 1 nm below the fundamental laser wavelength after time resolved spectra was acquired for each sample.

Biological Fluorophores

The biological fluorophores used for TRFS system validation were commercially available. These samples were Collagen type I from calf skin (C3511, Sigma-Aldrich), NADH (Nicotinamide Adenine Dinucleotide, N8129, Sigma-Aldrich) and FAD (Flavin Adenine Dinucleotide, F6625, Sigma-Aldrich). Collagen was tested in dry form whereas NADH and FAD were tested with PBS as the solvent. The solutions were diluted to the order of 10^{-6} M. The time resolved spectra of the biological fluorophores were obtained in

the same spectral range as the synthetic dyes. The temporal resolution during measurement for all the biological samples was set at 100 picoseconds.

Tissue Sample Validation

Several fresh human postmortem coronary arteries were used for this validation study. For the validation, the time-resolved fluorescence spectra were measured from the lumen side of the arteries, covering the spectral range between 400-600 nm. The scattered laser pulse temporal profile (instrument response) was also measured right after each time-resolved fluorescence spectrum acquisition.

RESULTS

Validation Results

The validation results for organic and biological fluorophores have been summarized in Tables 2 and 3. The emission spectra recorded using the TRFS system and the Impulse Response Functions (IRFs) obtained after deconvolution for the fluorescent dyes have been represented in Figures 8 (a) and 8 (b). Similarly, the emission spectra recorded using the TRFS system and the Impulse Response Functions (IRFs) obtained after deconvolution for the biological fluorophores have been represented in Figures 9 (a) and 9 (b). The lifetimes were calculated using a novel algorithm for Laguerre deconvolution developed in the laboratory. Peak wavelengths in the emission spectra of each sample were chosen for deconvolution. Tables 2 and 3 demonstrate the agreement between lifetime values obtained through Laguerre deconvolution with those in the literature for each fluorophore sample. This shows the robustness of Laguerre deconvolution technique for short lifetime (Rose Bengal) as well as longer lifetime (9CA) samples. Figure 10 and 11 show the steady state emission spectra and IRF at peak wavelength respectively for a coronary human artery sample that was used for validation. Based on the low residual level for the deconvolution, it can be observed that the Laguerre method successfully deconvolved the artery TRFS data. The lifetime values obtained from the arterial TRFS data ranged from ~1.5-3 ns, which are consistent with values reported in the literature.^{52, 53} The steady state spectra for these arterial samples show a broad emission band with peak emission between 400-450 nm, which suggests high Collagen/Elastin content in the arteries.

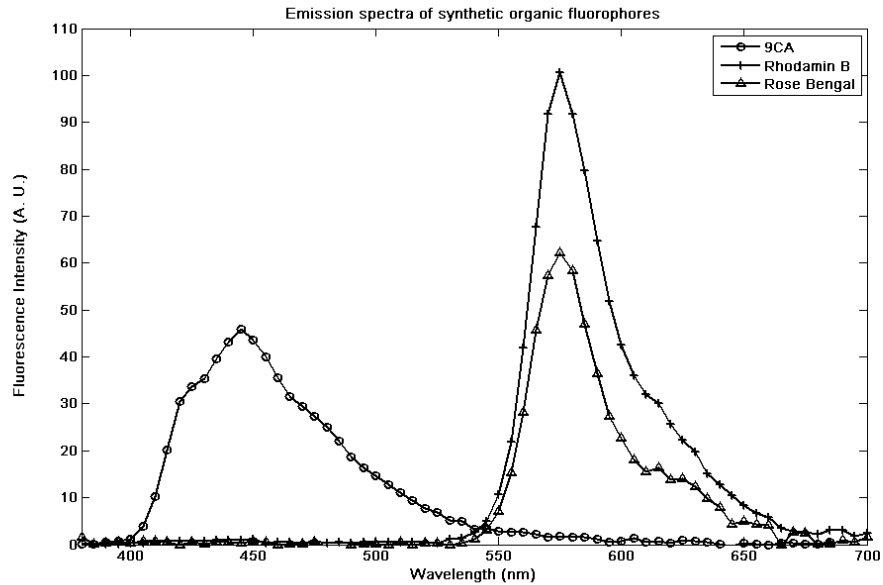


Figure 8 (a): Emission spectra of fluorescent dyes

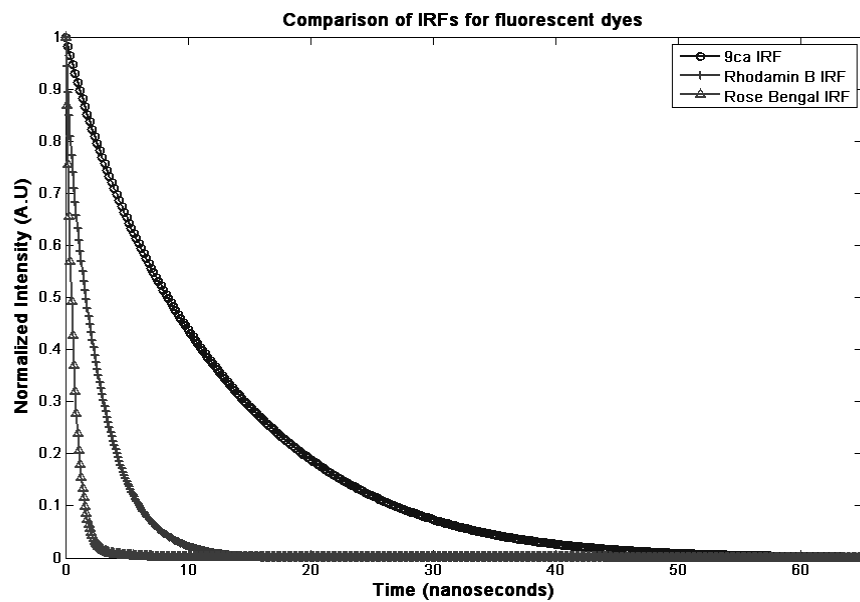


Figure 8 (b): Deconvolved Impulse Response Functions (IRFs) of fluorescent dyes

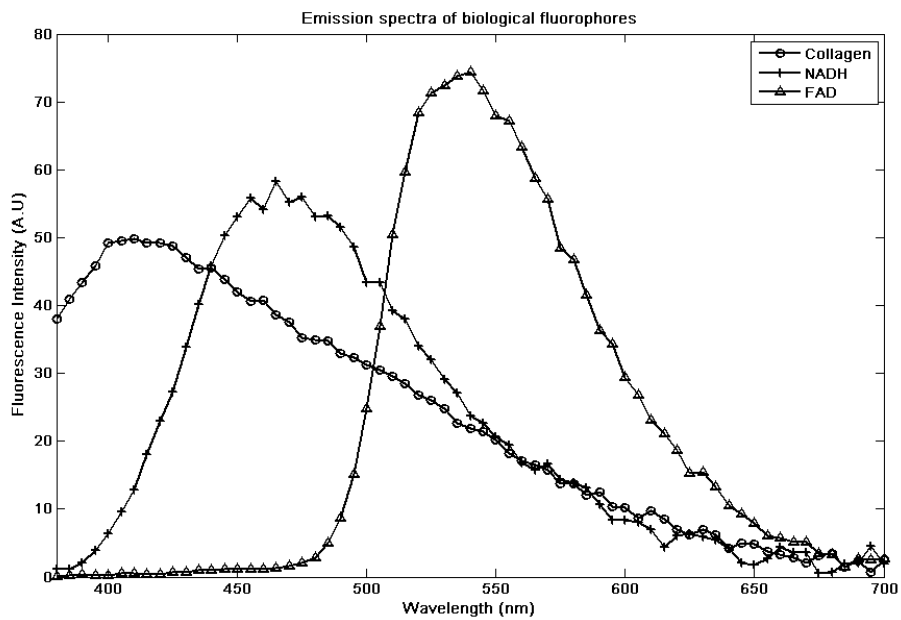


Figure 9(a): Emission spectra of biological fluorophores

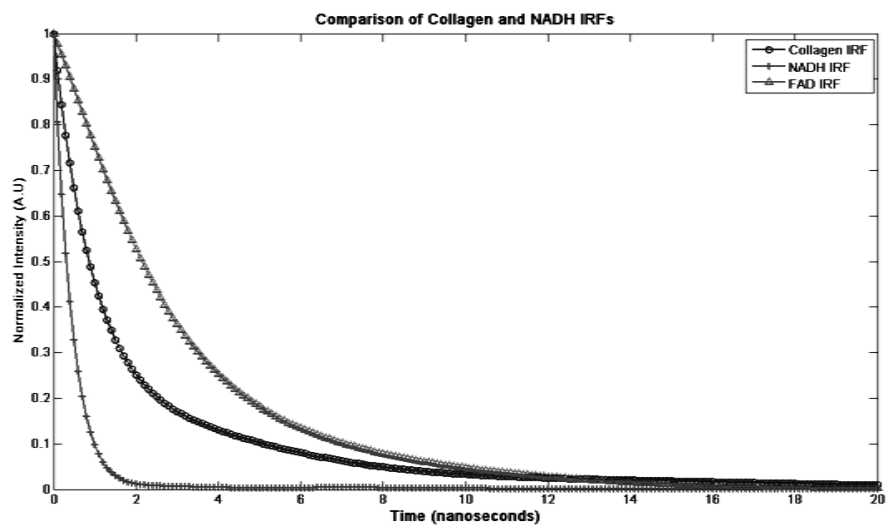


Figure 9(b): Deconvolved Impulse Response Functions (IRFs) of biological fluorophores

Table 2: Peak wavelengths and fluorescence lifetime values of fluorescent dyes

Sample	Solution	Peak wavelength (nm)	Lifetime (ns)	
			Laguerre deconvolution	Lifetime (ns) Literature
9CA	Ethanol	444	12.61 +/- 0.58	11.7 – 12.28
Rhodamin B	Ethanol	580	2.52 +/- 0.10	2.60 – 3.01
Rhodamin B	H ₂ O	580	1.55 +/- 0.03	1.48 – 1.67
Rose Bengal	Ethanol	570	0.65 +/- 0.02	0.84 – 0.85
Rose Bengal	Methanol	570	0.48 +/- 0.01	0.54 – 0.655

Table 3: Peak wavelengths and fluorescence lifetime values of fluorescent biomolecules

Sample	Solution	Peak wavelength (nm)	Lifetime (ns)	
			Laguerre Deconvolution	Lifetime (ns) Literature
Collagen	Dry	400	3.49 +/- 0.14	2.0 – 4.0
NADH	PBS	450	0.45 +/- 0.03	0.30 – 0.50
FAD	PBS	530	3.11 +/- 0.13	3.0 – 4.0

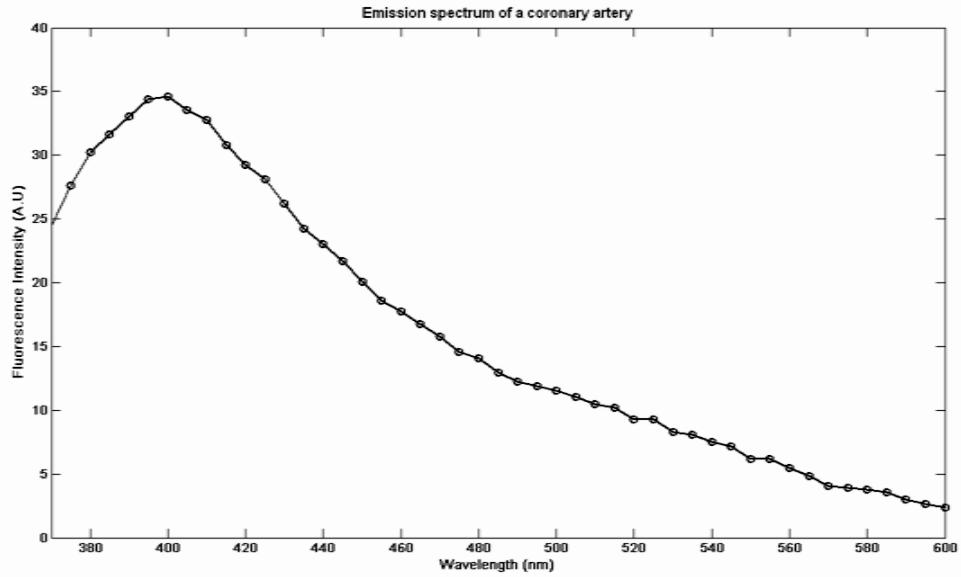


Figure 10: Steady state emission spectra of a coronary artery sample

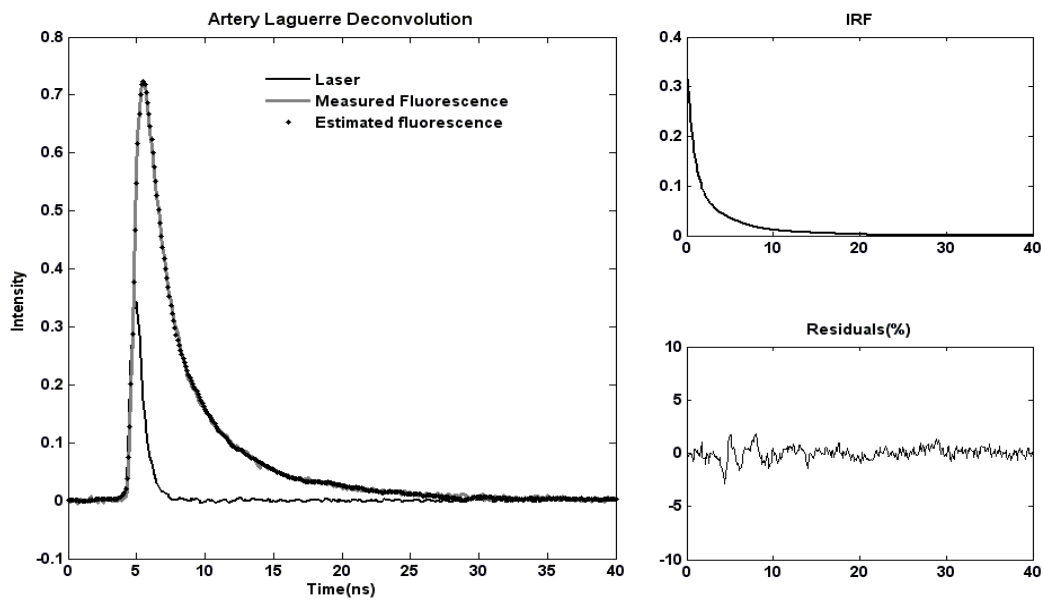


Figure 11: Deconvolution results for a fluorescence decay at 400 nm from an arterial sample

System Performance

Table 4 summarizes and compares the acquisition speed, data processing speed and deconvolution results for the TRFS system using two different light sources (337 nm, 1 ns nitrogen laser and 355 nm, 1.3 ns diode pumped semiconductor laser). Both light sources are UV pulsed lasers and hence capable of exciting the biological fluorophores present in the tissue. The MNL 200 nitrogen laser was operated at its maximum repetition rate (50 Hz) during acquisition. The TRFS system when utilizing the nitrogen laser as the light source, acquired a spectrum of about 40 wavelengths in ~19 seconds suggesting a rapid acquisition speed of about 400-500 ms per wavelength. All the signals were averaged 16 times before acquisition to ensure a good signal to noise ratio. A single wavelength acquisition took ~ 400 ms.

Table 4: Comparison of deconvolution results between 337 nm, 1 ns nitrogen & 355 nm, 1.3 ns Diode lasers

Sample	Solution	Peak wavelength (nm)	Lifetime (ns)	
			Laguerre Deconvolution (337 nm, 1.0 ns IR)	Laguerre Deconvolution (355nm, 1.3 ns IR)
9CA	Ethanol	445	12.61	12.66
Rhodamin B	Ethanol	580	2.52	2.77
Rose Bengal	Ethanol	570	0.65	0.63
NADH	PBS	450	0.45	0.54
FAD	PBS	530	3.11	3.16

A diode pumped laser (SPOT, ELFORLIGHT) was the other light source that was tested with the TRFS system. The SPOT laser (355 nm, 1.3 ns) had a comparatively broader bandwidth but could operate at a high repetition rate. During acquisition, the laser was operated at 5 KHz. At this repetition rate, the TRFS system acquired a spectrum of 40 wavelengths in ~ 15 seconds. This suggested an improvement in the acquisition speed at higher repetition rates. A single wavelength acquisition took ~ 250 ms.

An online Laguerre deconvolution algorithm was implemented in MathScript™, LabVIEW and was integrated into the TRFS system GUI. The algorithm could deconvolve at discrete wavelengths or deconvolve the entire time resolved spectrum at a time. The deconvolution algorithm took approximately 1 second for each discrete wavelength. An ultrafast matrix deconvolution approach was used for the analysis of time resolved spectra and hence the algorithm could deconvolve a spectrum of about 40 wavelengths in a little less than 6 seconds. Table 5 summarizes the system performance results.

Table 5: System performance results

Light Source	Repetition rate (Hz)	Time for single decay acquisition (ms)	Time for spectral acquisition, 200 nm in steps of 5 nm (seconds)
MNL nitrogen laser			
337 nm, 1.0 ns	50	~ 400	~ 19
SPOT laser			
355 nm, 1.3 ns	5000	~ 250	~ 15

CONCLUSION, DISCUSSION AND FUTURE WORK

The design of a versatile Time Resolved Fluorescence Spectroscopy (TRFS) apparatus compatible with clinical diagnostic applications has been reported here. The TRFS system can acquire time resolved fluorescence spectra from in vitro and ex vivo samples and can be used for in vivo applications as well. The system was validated using fluorescent dyes, biological fluorophores and tissue samples from human coronary arteries. Both steady state spectra and lifetime values were found to be in agreement with previously published work.⁴⁹

The goal in designing the TRFS system was to enable rapid real-time acquisition of time resolved data and near-real time data analysis. Near real-time data acquisition was accomplished by applying the pulse sampling technique for acquiring fluorescent decays and using a high speed digitizer/oscilloscope for sampling the data. The scope also served the dual purpose of a computer workstation. All system components were interfaced to the computer and automated as well as synchronized for smooth system operation. The system was designed flexibly so as to accommodate different light sources as well as different fiber optic probes. Both light sources were capable of exciting most of the biological fluorophores. The MNL 200 nitrogen laser along with the attached dye module would be useful for clinical applications that also involve exogenous fluorophores since it has the capability to excite the samples over a broad range. The SPOT diode pumped Q-switched high repetition laser was also found to be appropriate for tissue fluorescence measurements. It was capable of performing acquisitions at a high repetition rate (~5 KHz) and hence increased the system's acquisition speed, consequently reducing acquisition times. Although it had a broader pulse width (~1.3 nanoseconds) as compared

to the MNL 200 nitrogen laser (1 nanosecond), data acquired was successfully deconvolved with high accuracy (Table 4) even for dyes with short lifetimes (Rose Bengal). The SPOT laser had a lower energy per pulse as compared to the MNL 200 nitrogen laser. However, operation at high repetition rates meant more average power and hence time resolved fluorescence data was acquired even for low signal samples (i.e. low concentration/low quantum yield fluorophores) with a good signal to noise ratio. Two fiber optic probes were tested with the TRFS system. The fiber optic bundle was versatile and could be used for in vivo, ex vivo as well as in vitro applications. The side looking single fiber setup was found to be appropriate for in vivo applications.

Table 6: Comparison of the present TRFS system with previous studies

Group	Time domain approach	Acquisition time	Resolution	Data analysis approach
Glanzzman et al	Streak camera	20 seconds, 200 nm spectra, steps of 10 nm	1 nm spectral 10 ps temporal	LSIR
Pitts et al	Pulse sampling	Less than 1 sec per decay	3 nm spectral 300 ps temporal	LSIR
Fang et al	Pulse sampling	20 seconds, 200 nm spectra, steps of 5 nm	0.5 nm spectral 100 ps temporal	Laguerre deconvolution
Manning et al	TCSPC	---	---	LSIR
Present Study	Pulse sampling	15 seconds, 200 nm spectra, steps of 5 nm	0.5 nm spectral, 25 ps temporal	Online Laguerre deconvolution

Time resolved fluorescence studies have been applied to the investigation of several diagnostic problems. However, it has been difficult to translate the technology to the clinic mainly because of slow acquisition speed and the need for offline data analysis. Several design aspects of the TRFS system have been improved over previously reported systems to enable its implementation as a clinical tool (Table 6). The system is capable of acquiring time resolved spectra at high temporal (as low as 25 picoseconds) and high spectral resolution (as low as 0.5 nm). The acquisition speed (250 ms for a single fluorescence decay and ~ 15 seconds for a 200 nm spectrum in steps of 5 nm) is an improvement over previous acquisition times that have been reported. Although, several data analysis techniques have been employed for rapid data analysis in time resolved fluorescence spectroscopy, data analysis has always been done offline. This is the first time ever that an online near-real time data analysis technique has been implemented and integrated with the TRFS system GUI. The time taken for online data analysis (~ 1 second for deconvolving a single fluorescence decay and ~ 5 seconds for deconvolving a 200 nm spectrum) of time resolved data seems adequate for clinical applications. Table 6 presents a brief comparison of the present system capabilities with TRFS systems that have been developed previously.

In summary, a novel portable and versatile Time Resolved Fluorescence Spectroscopy (TRFS) apparatus for near-real time diagnosis in clinical applications was designed and implemented. The TRFS system is being applied in the laboratory for investigating the biochemical composition of atherosclerotic plaques, and will eventually be utilized for in vivo clinical detection of vulnerable plaques that pose fatal risk to a

patient. The system versatility could also promote its applications to cancer detection or other regular diagnostic procedures.

REFERENCES

1. J. R. Lakowicz, Principles of Fluorescence Spectroscopy, Third Edition, Springer, Berlin (2006)
2. M. Kobayashi, R. Sawada, and Y. Ueda, IEEE Journal of Selected Topics in Quantum Electronics, **9**(2), (2003)
3. M. Anidjar, O. Cussenot, S. Avrillier, D. Etori, P. Teillac, and A. Le Duc, Annals of New York Academy of Sciences, **838**, 130-42, (1998)
4. G. M. Palmer, P. J. Keely, T. M. Breslin and N. Ramanujam, Photochemistry and Photobiology, **78**(5), 462–469, (2003)
5. L. Brancalion, A. J. Durkin, J. H. Tu, G. Menaker, J. D. Fallon and N. Kollias, Photochemistry and Photobiology, **73**(2), 178–183, (2001)
6. G. Zonios, R. M. Cothren, J. Arendt, J. Wu, J. M. Crawford, J. Van Dams, R. Manoharan and M. S. Feld, Proceedings of SPIE, **2324**, 9 (1995)
7. R. S. DaCosta, B. C. Wilson and N. E. Marcon, Clinical Gastroenterology, **20**(1), 41-57 (2006)
8. Wei-Chiang Lin, S. A. Toms, M. Johnson, E. Duco Jansen and A. Mahadevan-Jansen, Photochemistry and Photobiology, **73**(4), 396 – 402, (2001)
9. A. Gillenwater, R. Jacob, R. Ganeshappa, B. Kemp, A. K. El-Naggar, J. L. Palmer, G. Clayman, M. F. Mitchell, R. Richards-Kortum, Archives of Otolaryngology, Head & Neck Surgery, **124**, (1998)
10. S. Andersson-Engels, J. Johansson, U. Stenram, K. Svanberg and S. Svanberg, IEEE Journal of Quantum Electronics, **26**(12), 2207–2217, (1990)

11. N. Ramanujan, Encyclopedia of Analytical Chemistry, John Wiley & Sons, R.A. Meyers (Ed.), 20–56, (2000)
12. A.E. Saarnak, T. Rodrigues, J. Schwartz, A.L. Moore, T.A. Moore, D. Gust, M.J.C. van Gemert, H.J.C.M. Sterenborg and S. Thomsen, Lasers in Medical Science, **13**, 22-31 (1998)
13. T. Glanzmann, J. P. Ballini, H. van den Bergh, and G.Wagnieres, Review of Scientific Instruments, **70**, 4067 (1999)
14. J.D Pitts and Mary Ann Mycek, Review of Scientific Instruments, **72**(7) (2001)
15. H. B. Manning, G. T. Kennedy, D. M. Owen, D. M. Grant, A. I. Magee, M. A. A. Neil, Y. Itoh, C. Dunsby and P. M.W. French, Journal of Biophotonics, **1**(6), 494 – 505 (2008)
16. M.A. Mycek, K.T. Schomacker, N.S. Nishioka, Gastrointestinal Endoscopy, **48**(4), (1998)
17. Hsin-Ming Chen, Chun-Pin Chiang, Chun You, Tzu-Chien Hsiao, and Chih-Yu Wang, Lasers in Surgery and Medicine, **37**, 37–45 (2005)
18. L. Marcu, Q. Fang, J. Jo, T. Papaioannou, A. Dorafshar, T. Reil, Jian-Hua Qiao, J. Dennis Baker, J. A. Freischlag and M. C. Fishbein, Atherosclerosis, **181**(2), 295-303 (2005)
19. L. Marcu, J. A. Jo, Q. Fang, T. Papaioannou, T. Reil, Jian-Hua Qiao, J. Dennis Baker, J. A. Freischlag and M. C. Fishbein, Atherosclerosis, **204**(1), 156-64 (2008)
20. W. H. Yong, P. V. Butte, B. K. Pikul, J. A. Jo, Q. Fang, T. Papaioannou, K. Black, L. Marcu, Frontiers in Bioscience, **11**, 1255-1263, (2006)
21. Jablonski Energy Diagram, Accessed on 20th February 2009

(<http://www.shsu.edu/~chemistry/chemiluminescence/JABLONSKI.html>)

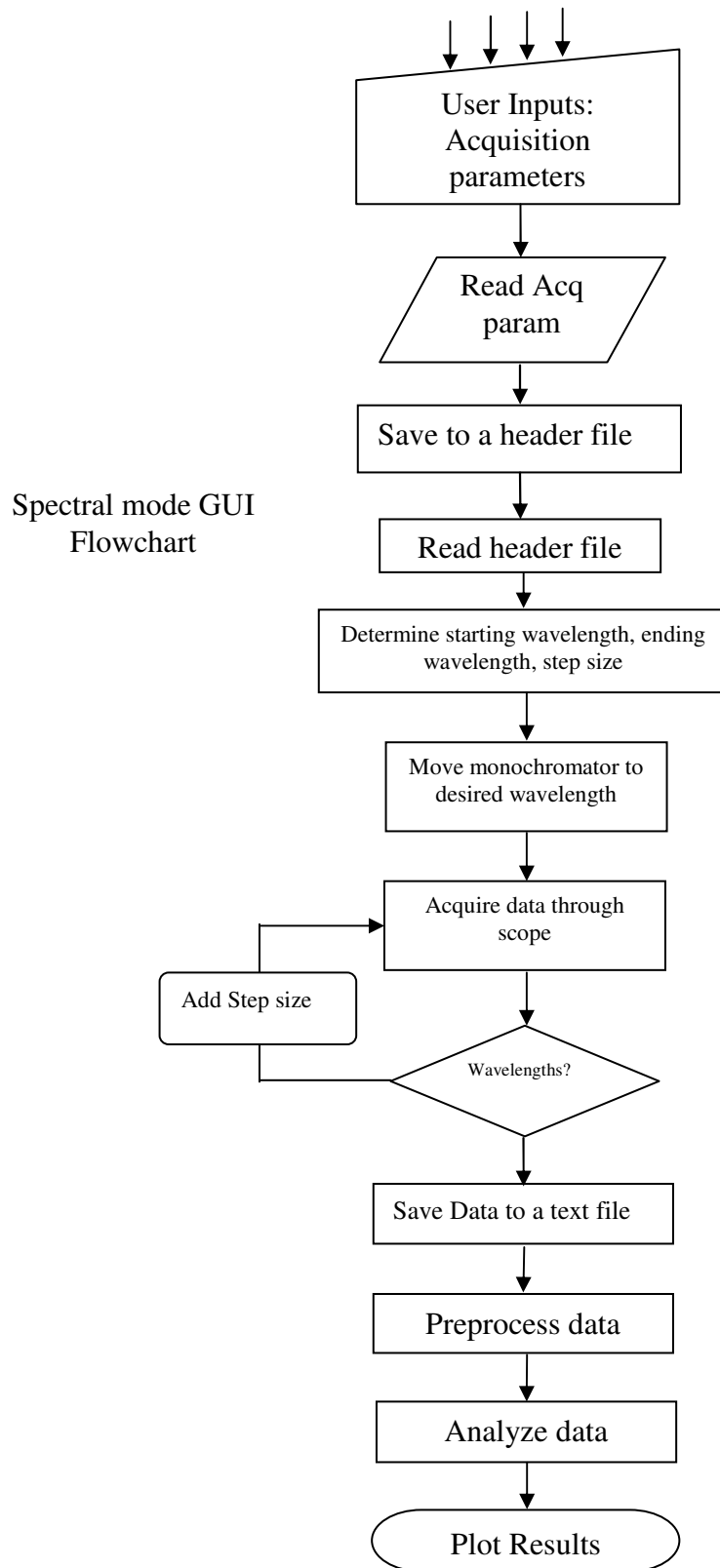
22. R. Richards-Kortum and E. Sevick-Muraca, *Annual Review of Physical Chemistry*, **47**, 555–606, (1996)
23. M. J. Davies, *Circulation*, **94**(8), 2013-20 (1996)
24. P. K. Shah, E. Falk, J. J. Badimon, A. Fernandez-Ortiz, A. Mailhac, G. Villareal-Levy, J. T. Fallon, J. Regnstrom and V. Fuster, *Circulation* **92**, 1565-1569 (1995)
25. D.R. Eyre and M.A. Paz, *Annual Review of Biochemistry*, **53**, 717–748 (1984)
26. D.P. Thornhill, *Biochemical Journal*, **147**, 215–219 (1975)
27. B. Valeur, *Molecular Fluorescence – Principles and Applications*, Wiley InterScience (2001)
28. J. Lippincott-Schwartz, E. Snapp, A. Kenworthy, *Nature Reviews Molecular Cell Biology* **2**, 444-456 (2001)
29. W.M. Vaughan, & G. Weber, *Biochemistry*, **9**,464-473. (1970)
30. G. A. Wagnieres, W. M. Star and B. C. Wilson, *Photochemistry and Photobiology*, **68**(5), 603-632, (1998)
31. E. Strackle, C. Blum, S. Becker, K. Mullen and A. J. Meixner, *ChemPhysChem*, **6**, 1242-1246 (2005)
32. J. R. Lakowicz and G. Weber, *Biochemistry*, **12**, 4161 (1973)
33. F. Dorr, *Mechanisms of Energy Transfer, Biophysics*, Springer-Verlag, Berlin, 265 – 288 (1983)
34. S. Anderssonengels, J. Johansson, K. Svanberg, and S. Svanberg, *Photochemistry and Photobiology*, **53**, 807 (1991)

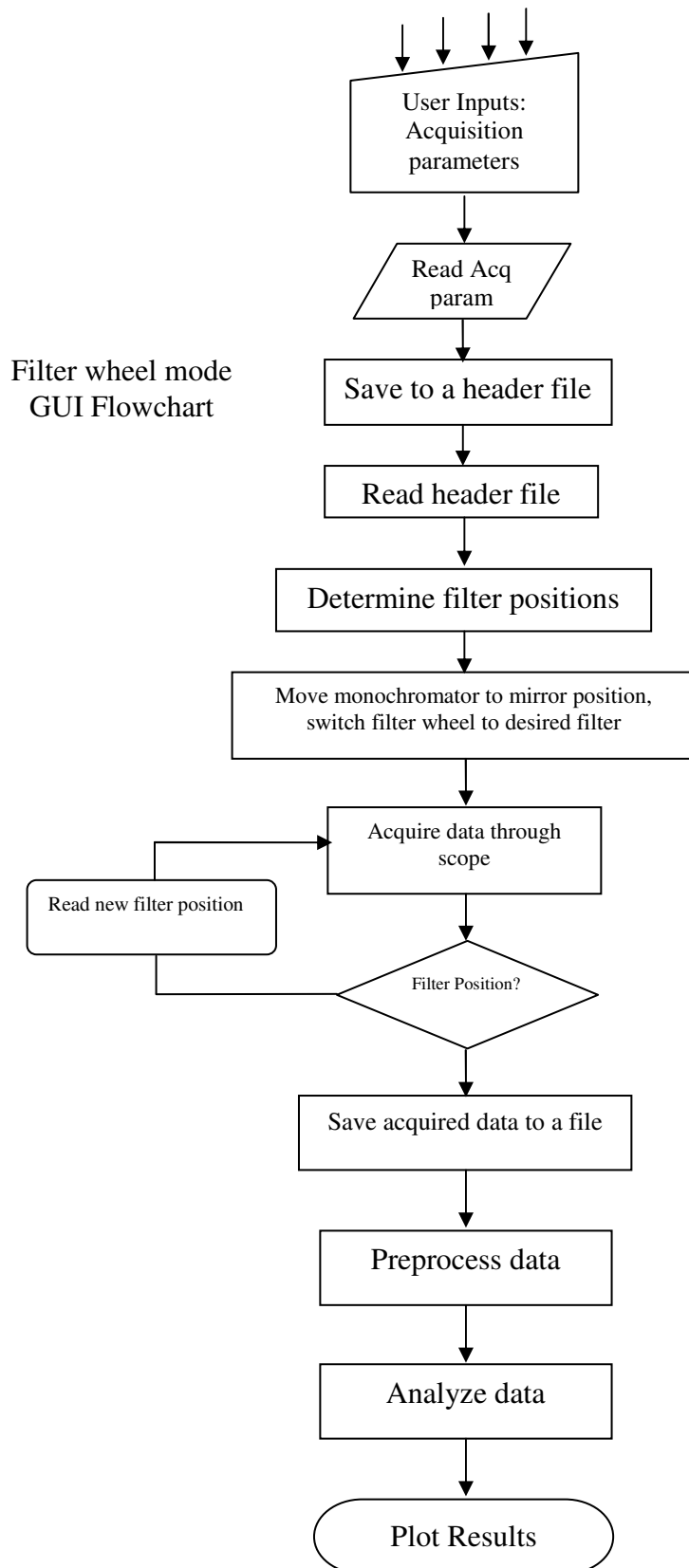
35. J. Gregoire, W. D. Edwards, M. H. Jeong, A. R. Camrud, A. Lerman, R. A. VanTassel, K. R. Bailey, D. R. Holmes, and R. S. Schwartz, *Lasers in Surgery and Medicine*, **21**, 374 (1997)
36. J. M. I. Maarek, L. Marcu, W. J. Snyder, and W. S. Grundfest, *Photochemistry and Photobiology*, **71**, 178 (2000)
37. L. Marcu, W. S. Grundfest and J. M. I. Maarek, *Photochemistry and Photobiology*, **69**(6): 713-721 (1999)
38. C. Deka, B.E. Lehnert, N.M. Lehnert, G.M. Jones, LA. Sklar, and JA. Stelnkamp, *Cytometry* **25**, 271-279 (1996)
39. D. J.S. Birch, A. Ganesan and Jan Karolin, *Synthetic Metals* 155 (2005) 410–413
40. S. Draxler and M. E. Lippitsch, *Analytical Chemistry*, **68**(5), 753–757 (1996)
41. J. R. Lakowicz, G. Laczko, H. Cherek, E. Gratton and M. Limkeman, *Biophysical Journal*, **46**, 463-477 (1984)
42. Fluorescence lifetime measurement principles, Accessed on 26th February 2009 (<http://www.olympusfluoview.com/applications/images/flimfigure1.jpg>)
43. J. R. Lakowicz, H. Szmzinski and I. Gryczynski, *Photochemistry and Photobiology*, **47**(1), 31 – 41 (1988)
44. E. Gratton, D.M. Jameson, R.D. Hall, *Annual Review of Biophysics & Bioengineering*, **13**(105), (1984)
45. D. Elson, J. Requejo-Isidro, I. Munro, F. Reavell, J. Siegel, K. Suhling, P. Tadrous, R. Benninger, P. Lanigan, J. McGinty, C. Talbot, B. Treanor, S. Webb, A. Sandison, A. Wallace, D. Davis, J. Lever, M. Neil, D. Phillips, G. Stamp and P. French, *Photochemistry and Photobiology Sciences*, **3**, 795–801 (2004)

46. W. Becker, A. Bergmann, G. L. Biscotti, and A. Rueck, *Proceedings of SPIE*, **5340**, 104-112 (2004)
47. A. C. Mitchell, J. E. Wall, J. G. Murray and C. G. Morgan, *Journal of Microscopy*, **206**(3), 233 – 238 (2002)
48. A. C. Bühler, U. Graf, R. A. Hochstrasser, M. Anliker, *Review of Scientific Instruments*, **69**(3), 1512-1518 (1998)
49. J. M. Maarek, L. Marcu, M. Fishbein, W. S. Grundfest, *Lasers in Surgery and Medicine*, **27**, 241-254, (2000)
50. Q. Fang, T. Papaioannou, J. A. Jo, R. Vaitha, K. Shastry and L. Marcu, *Review of Scientific Instruments*, **75**(1), (2004)
51. D. V. O'Connor and D. Phillips, *Time-Correlated Single-Photon Counting*, Academic Press, New York (1984)
52. L. Marcu, Q. Fang, J. A. Jo, T. Papaioannou, A. Dorafshar, T. Reil, Jian-Hua Qiao, J. Dennis Baker, J. A. Freischlag, M. C. Fishbein, *Atherosclerosis*, **181**, 295–303 (2005)
53. P. V. Butte, B. K. Pikul, A. Hever, W. H. Yong, K. L. Black, L. Marcu, *Journal of Biomedical Optics*, **10**(6), 064026-1 - 064026-9 (2005)
54. W. Georges, M. Jerome, A. Studzinski, H. van den Bergh, *Proceedings of SPIE*, **2392**, 42-54 (1999)
55. F. V. Bright and C. A. Munson, *Analytica Chimica Acta*, **500**, 71–104 (2003)
56. J. R. Lakowicz, *Principles of Fluorescence Spectroscopy*, 3rd edition, Chapter 4, Springer, Berlin (2006)
57. J. A. Jo, Q. Fang, T. Papaioannou and L. Marcu, *Journal of Biomedical Optics*, **9**(4), 743–752 (2004)

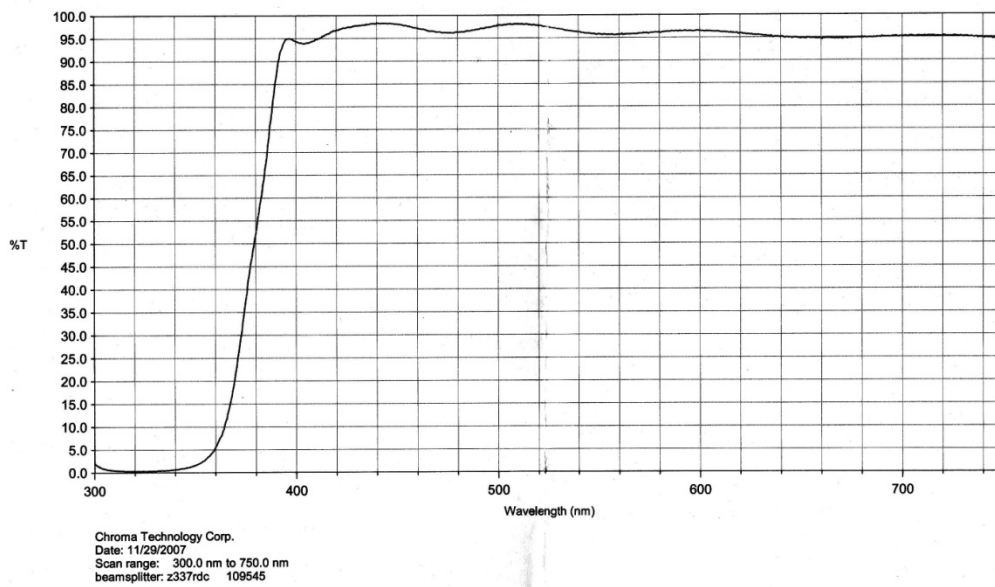
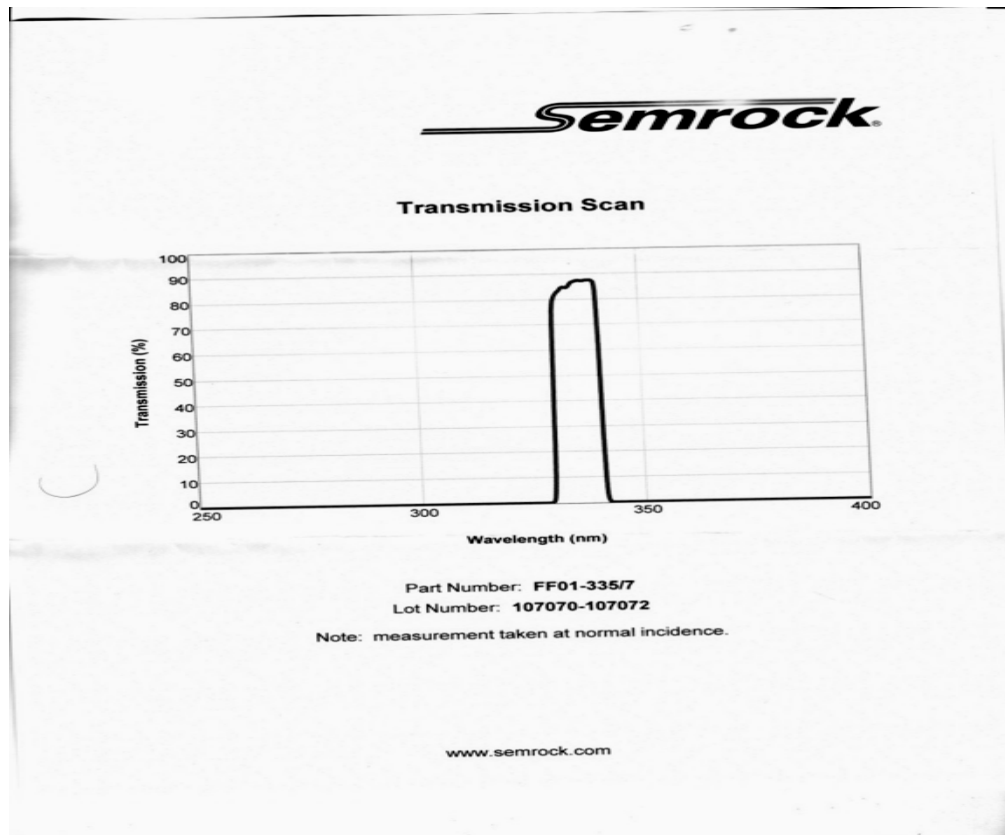
58. A. Volkmer, D. A. Hatrick and D. J. S. Birch, *Measurement Science & Technology*, **8**, 1339–1349 (1997)
59. W. R. Ware, L. J. Doemeny, and T. L. Nemzek, *Journal of Physical Chemistry*, **77**, 2038–2048 (1973)
60. A. Grinvald and I. Z. Steinberg, *Analytical Biochemistry*, **59**, 583–598 (1974)
61. M. L. Johnson and S. G. Frasier, *Methods in Enzymology*, **117**, 301–342 (1985)
62. D. V. O'Connor and W. R. Ware, *Journal of Physical Chemistry*, **83**, 1333–1343 (1979)
63. A. Gafni, R. L. Modlin, and L. Brand, *Biophysical Journal*, **15**, 263–280 (1975)
64. K. C. Lee, J. Siegel, S. E. D. Webb, S. Leveque-Fort, M. J. Cole, R. Jones, K. Dowling, M. J. Lever, and P. M. W. French, *Biophysical Journal*, **81**, 1265–1274 (2001)
65. J. M. Beechem, E. Gratton, J. M. Ameloot, J. R. Knutson, and L. Brand, *Topics in Fluorescence Spectroscopy, Vol. 2, Principles*, J. R. Lakowicz, Ed., Plenum Press, New York (1991)
66. J. M. Maarek, L. Marcu, W. J. Snyder, and W. S. Grundfest, *Photochemistry and Photobiology*, **71**, 178–187 (2000)

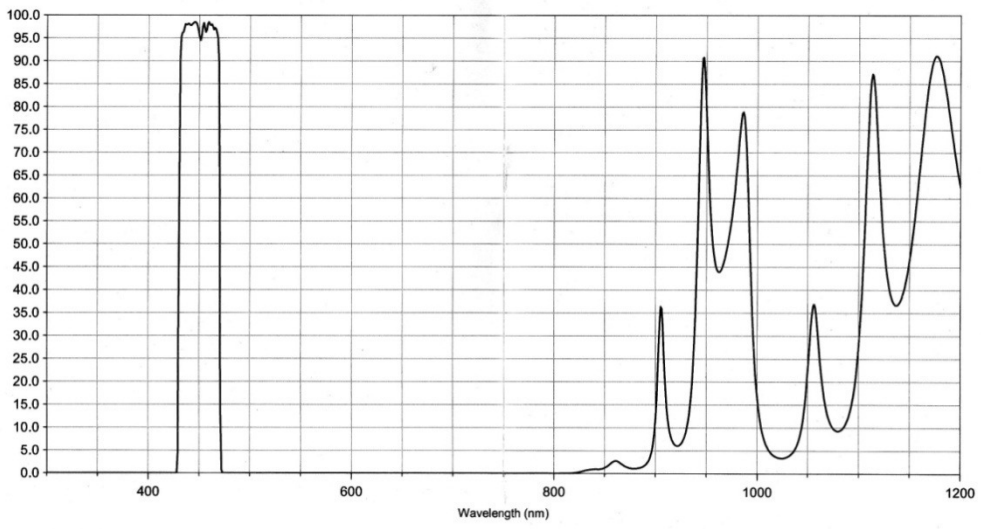
APPENDIX A: FLOW CHARTS FOR TRFS GUI



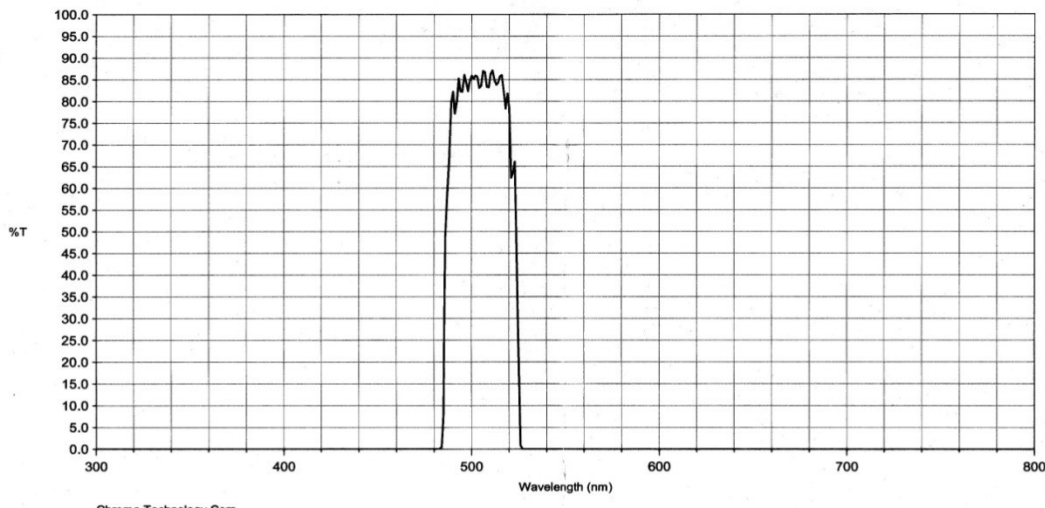


APPENDIX B: FILTER RESPONSES





Chroma Technology Corp.
Date: 11/29/2007
Scan range: 300.0 nm to 1200.0 nm
emitter: ET450/40 118727

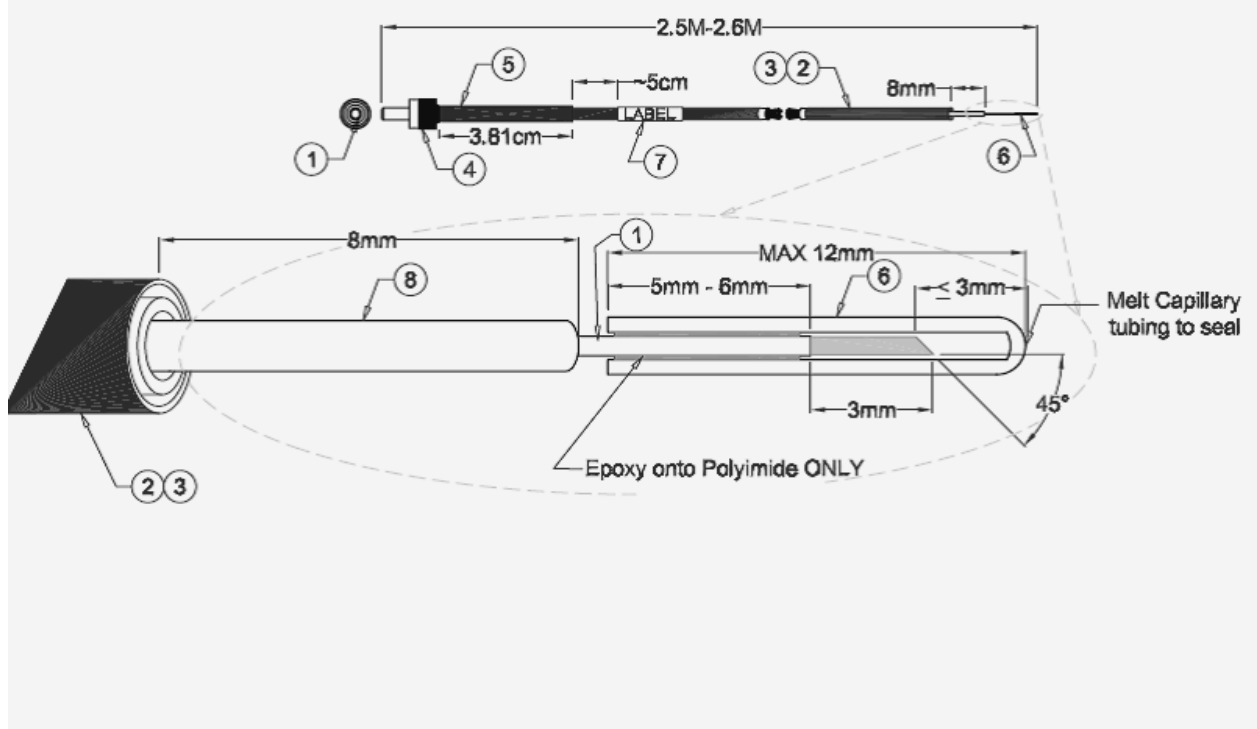
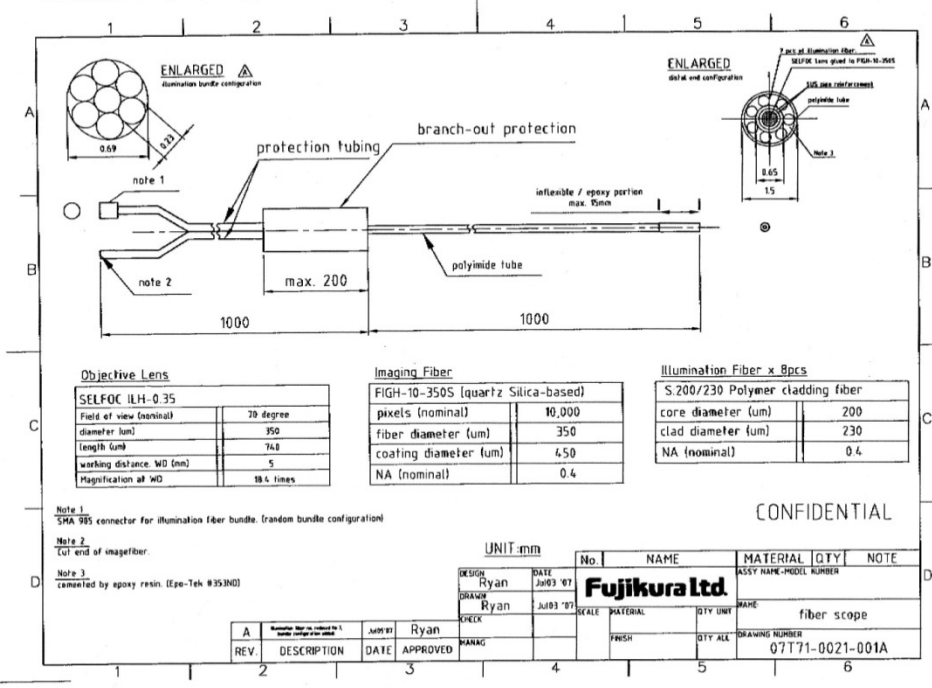


Chroma Technology Corp.
Date: 11/29/2007
Scan range: 300.0 nm to 800.0 nm
emitter: HQ505/40 53606

APPENDIX C: FIBER DESIGNS

P. 02
 FAX NO. 864 486 7272
 JUL-05-2007 THU 04:11 PM AFL TELECOMMUNICATIONS

This drawing must not be passed onto any person not authorized by us to receive, send nor copied or otherwise made used of by such a person without our authority.



VITA

Name: Chintan A. Trivedi

Address: 145 Wisenbaker Engineering Research Center

College Station, Texas – 77843

Email: chintan_bme@tamu.edu

Education: Bachelor of Engineering, Biomedical & Instrumentation

Saurashtra University, India, 2006